Pergamon

0890-4332(94)00055-7

Heat Recovery Systems & CHP Vol. 15, No. 5, pp. 389–423, 1995

0890-4332/95 $9.50 + .00

REVIEW PAPER

ELECTROHYDRODYNAMIC ENHANCEMENT OF HEAT TRANSFER AND FLUID FLOW

P. H. G. ALLEN* and T. G. KARAYIANNIS†‡

*Thermo-Fluids Engineering Research Centre, City University, London, EC1V OHB, UK; and
†School of Engineering Systems and Design, South Bank University, London, SE1 0AA, UK

(*Received* 1 *July* 1994)

Abstract—The electrohydrodynamic (EHD) enhancement mechanism is first outlined in this paper. A comprehensive review of past work on EHD single and two-phase heat transfer, as well as past work in the related area of EHD-induced flow, is then presented. Correlation attempts are also reviewed. Recent experimental results for EHD boiling and condensation in single- and multi-tube heat exchangers are discussed. A description of the possible practical EHD electrode systems for applications in power production cycles and refrigeration is also presented. The research work needed to clarify outstanding questions in EHD and encourage its use in practical systems is discussed.

NOTATION

A	dimensionless group (see equation (33))
B	dimensionless group (see equation (50))
C_A, C_B, C_C	empirical constants
C_p	specific heat (J/kg K)
d	vapour film thickness (m)
D	diameter (m) total differential operator
D_c	charge diffusion coefficient (m^2/s)
E	electric field strength (V/m)
El	electric influence number (defined in equation (31))
El'	electric influence number (defined in equation (34))
f_1, f_2	defined in equations (47) and (49) (FV^2/m^2)
f	frequency (Hz)
F_b	buoyancy force (N)
F_d	dielectrophoretic force on bubbles defined in equation (22) (N)
F_D	body force comprising second and third term of equation (1) (N/m^3)
F_E	electrohydrodynamic body force defined in equation (1) (N/m^3)
$F_{\tilde{c}}$	equivalent EHD force (defined in equation (39)) (N/m^3)
g	acceleration due to gravity (m/s^2)
G	dimensionless group (see equation (50))
h	surface height (m)
i	current (A)
i_{lg}	enthalpy of evaporation (J/kg)
$\Delta i'$	thermal energy term (defined in equation (40)) (J/kg)
J	current density (A/m^2)
K	dimensionless group (defined in equation (42))
ℓ	characteristic length (m)
L	length (m)
n	empirical exponent
Ne	dimensionless group (defined in equation (35))
N	dimensionless group (defined in equation (52))
Nu	Nusselt number ($Nu = a\ell/\lambda$)
Nu'	modified Nusselt number (defined in equation (37))
ΔNu	change in Nu
P	pressure (N/m^2)
P_e	electric power input (W)
Pr	Prandtl number ($Pr = \mu c_p/\lambda$)
Q	thermal throughput (W)
q	electric charge density (C/m^3)

‡Author to whom correspondence should be addressed.

ΔQ	change in Q (W)
$\dot{q}$	thermal flux density (W/m^2)
R, r	radius (m)
$\bar{r}$	unit radial vector
Ra'	modified Rayleigh number (defined in equation (38))
Re	Reynolds number ($Re = vl/\nu$)
Re'	dimensionless group (defined in equation (44))
Re_0	dimensionless group (defined in equation (53))
Re'_E	dimensionless group (defined in equation (45))
t	time (s)
T	temperature (C)
ΔT	temperature difference, wall-saturated vapour, wall-bulk fluid (K)
v	fluid velocity (m/s)
V	volume flowrate (m^3/s)
V_R	reactor power (kW)

Greek letters

α	heat transfer coefficient (W/m^{2}K)
α'	corrected (condensation) heat transfer coefficient (W/m^{2}K)
β	fluid coefficient of cubic expansion (1/K)
ϵ	fluid permittivity (F/m)
$\varkappa$	thermal diffusivity (m^2/s)
μ	dynamic viscosity (Ns/m)
θ	contact angle (rad)
λ	thermal conductivity (W/mK)
λ^*	perturbation wavelength (m)
η	ion mobility (m^2/V s)
ν	kinematic viscosity (m^2/s)
π	dimensionless group (defined in equation (43))
ϱ	density (kg/m^3)
σ	surface tension (N/m)
σ_e	electrical conductivity (S/m)
τ	charge relaxation time (s)
ϕ	velocity (V)

Superscripts

–	mean, indicates vector quantity

Subscripts

c	corona, critical
D	dielectrophoretic plus electrostrictive
E	due to electric field
g	saturated vapour
gw	vapour to solid
i	inner
l	liquid
lg	liquid to vapour
ln	logarithmic mean
max	maximum
min	minimum
o	outer
0	of free space (permittivity), at zero electric field
w	solid surface
wl	solid to liquid

1. INTRODUCTION

Achieving higher heat transfer rates through various enhancement techniques can result in substantial energy savings, due both to the increased performance of equipment and the design of smaller systems to meet required loads. A recent investigation into heat transfer enhancement initiated by the UK Energy Efficiency Office enumerated 20 different enhancement techniques [1].

In general, heat transfer enhancement methods are categorized as "passive" or "active", see Bergles [2, 3]. The first category includes the high heat-treated, rough or extended surfaces, displaced enhancement devices, additives, etc. The use of extended surfaces was the preferred technique in heat transfer enhancement in the past, both in single and in two-phase systems. In two-phase applications, manufacturers have recently introduced high heat flux surfaces. In boiling applications manufacturing techniques are employed to (a) deform the surface so as to create

re-entrant type cavities or (b) to deposit a matrix of metallic particles on the surface. Either gives a porous layer which enhances boiling by providing sites (the pores) for bubble generation. Bergles [2, 3] and Yilmaz *et al.* [4] provide experimental results on the performance of these high heat flux surfaces in boiling. In condensation applications, in addition to low fin tubes, tubes with sharp saw-tooth-type fins and trapezoidal-shaped extending fins are examples of enhanced tubes introduced more recently. The second category of enhanced methods includes techniques such as surface vibration, fluid vibration, vapour suction and a.c. or d.c. electrostatic fields.

The enhancement of single phase heat transfer processes, especially in gaseous systems, is an area where researchers and designers are spending a great deal of effort. The need to improve the heat transfer rates was made imperative by the ever increasing requirement for smaller, more cost-effective thermal systems. In single phase heat transfer, the boundary layers that form on the thermally-active surfaces offer a significant resistance to the flow of heat which in gaseous systems can dominate the resistance offered by the solid walls. Enhancing techniques are therefore employed to alter the boundary layer structure of the flow and, in laminar or free convective situations, to increase the flow velocity.

The phase change that occurs during a boiling and a condensation process is generally a very effective mode of heat transfer. However, there is further need to develop methods of enhancing the heat transfer rates in both evaporators and condensers. A refrigeration/heat pump system usually operates with heat sink and heat source at predetermined or not controllable (e.g. atmospheric) temperatures. The working fluid operating temperature must be significantly lower than the source and higher than the sink in order for the evaporator and the condenser to be of reasonable, economic size. In a refrigeration/heat pump system these temperature differences, which constitute external thermal irreversibility, reduce the coefficient of performance (COP) of the refrigerator or heat pump. Similar arguments hold for the power producing cycles where the efficiency of the cycle is reduced, as the greatest possible temperature difference is reduced by the external thermal irreversibility mentioned above.

The beneficial result of heat transfer enhancement, i.e. the increase in the heat transfer coefficient, would be:

(a) the reduction in the size of the heat exchangers for given ratings.

(b) the reduction in the temperature difference between the fluids exchanging heat and thus greater thermal plant efficiency. (Alternatively, the transfer of greater rates of energy through a given size of heat exchanger while maintaining moderate temperature differences.)

Reducing the temperature differentials at evaporator and condenser becomes particularly important in the more recent development of power production using ocean thermal energy conversion (OTEC) plants, geothermal energy plants, solar pond generation plants and similar plants utilizing the organic Rankine cycle (ORC). In these plants the available temperature difference (between source and sink) is already small, e.g. in OTEC plants this is the difference between the temperature of surface (20–30°C) and deep sea water (4–7°C). Plants operating between such small temperature differences must be significantly larger than high temperature plants (nuclear or fossil fuel plants) in order to produce similar outputs. In addition, their performance is more sensitive to the temperature differential at the evaporator-source and the condenser-sink. A certain degree of superheat must be exceeded in the evaporator for nucleate boiling to commence. Such plants may, therefore, face additional "start-up" problems if this degree of superheat is not available. This places an additional limitation on the maximum possible operating fluid temperature difference and thus reduces the plant efficiency.

The enhancing effect of a strong electric field on heat transfer rates (electrohydrodynamic—EHD—enhancement) has been known for over 70 yr. Early work concentrated on the enhancement of single-phase convective heat transfer. In the last 30 yr the greater potential of EHD in enhancing two-phase heat transfer rates has been realized by more industrial and academic researchers. This had led to the study of coupled electric field and pool boiling in the nucleate, transitional and film boiling regimes. The effect of the electric field on the peak nucleate and the minimum film boiling conditions has received particular attention. While work on EHD boiling proceeded steadily, relatively little was published on EHD condensation until the last decade, possibly due to the greater practical potential offered by EHD boiling. The present paper reviews

the published work on EHD enhanced single- and two-phase heat transfer and presents the results of recent work on both. A review of the past research on EHD-induced flow-pumping is also given for completeness.

2. EHD ENHANCEMENT MECHANISM

The physical basis of much electrically-enhanced heat transfer lies in the EHD force, F_E per unit volume, generated by an electric field, strength E, in a fluid of dielectric permittivity ϵ, density ϱ, at temperature T. This can be expressed as [5]

$$\bar{F}_E = q\bar{E} - \tfrac{1}{2}E^2\nabla\epsilon + \tfrac{1}{2}\nabla\left[E^2\left[\frac{\partial\epsilon}{\partial\rho}\right]_T\rho\right], \tag{1}$$

where q is the electric charge density in the fluid; $q\bar{E}$, its electrophoretic component, is the Coulomb force exerted by an electric field upon the free charge in it. The third term comprises the dielectrophoretic and electrostrictive forces on and within the fluid [6], due to the nature of $\bar{E}$ and ϵ and their spatial distribution.

Equation (1) should then be included in the Navier–Stokes equation which, for an incompressible fluid, is

$$\rho\frac{D\bar{v}}{Dt} = \rho\bar{g} + \bar{F}_E - \nabla P + \mu\nabla^2\bar{v}, \tag{2}$$

where $D\bar{v}/Dt$ denotes the substantive acceleration consisting of the local contribution $\partial\bar{v}/\partial t$ and the convective contribution $(\bar{v}\cdot\nabla)\bar{v}$. The vector $\rho\bar{g}$ is the gravitational force per unit volume; P is the local fluid pressure. The term $\mu\nabla^2\bar{v}$ represents the viscous terms.

For an incompressible fluid, the continuity equation is

$$\nabla\cdot\bar{v} = 0 \tag{3}$$

and the energy equation, neglecting viscous dissipation effects, is

$$\frac{\partial T}{\partial t} + \bar{v}\cdot\nabla T = \kappa\nabla^2 T + \frac{\sigma_e E^2}{\rho C_p}. \tag{4}$$

(The last term in equation (4) is the ohmic dissipation, which is usually neglected.)

For an ohmic dielectric, the electrostatic equations [7, 8] are

$$\nabla\cdot\epsilon\bar{E} = q \tag{5}$$

$$\nabla\times\bar{E} = 0 \tag{6}$$

$$\nabla\cdot\bar{J} + \frac{\partial q}{\partial t} = 0 \tag{7}$$

and $\bar{J}$ the current density is

$$\bar{J} = q\bar{v} + \sigma_e\bar{E} + (\bar{v}\cdot\nabla)(\epsilon\bar{E}) - D_e\nabla q. \tag{8}$$

Equations (2–8) will then formulate electroconvective problems.

In single-phase convective heat transfer, thermal gradients in the fluid produce non-uniformities in the electrical conductivity (σ_e) and the dielectric permittivity (ϵ). If there is a change of σ_e and ϵ in the fluid then free charge can build up, which can be acted upon by the electric field electrophoretic component of EHD force. The dependence of the free charge generation on the electrical conductivity and permittivity is given as follows.

Neglecting the movement of q, equation (8) becomes

$$\bar{J} = \sigma_e\bar{E}, \tag{9}$$

while in the steady state equation (7) becomes

$$\nabla\cdot\bar{J} = 0. \tag{10}$$

Then

$$\nabla \cdot J = \nabla \cdot (\sigma_e \bar{E}) = \bar{E} \cdot \nabla \sigma_e + \sigma_e \nabla \cdot \bar{E}, \tag{11}$$

which, for equation (10), gives

$$\sigma_e \nabla \cdot \bar{E} = -\bar{E} \cdot \nabla \sigma_e, \tag{12}$$

while, from equation (5),

$$\epsilon \nabla \cdot \bar{E} = q - \bar{E} \cdot \nabla \epsilon. \tag{13}$$

Dividing equation (13) by (12)

$$\frac{\epsilon}{\sigma_e} = \frac{q - \bar{E} \cdot \nabla \epsilon}{-\bar{E} \cdot \nabla \sigma_e}. \tag{14}$$

Rearranging equation (14) gives

$$q = \bar{E} \cdot \nabla \epsilon - \frac{\epsilon}{\sigma_e} \bar{E} \cdot \nabla \sigma_e. \tag{15}$$

(Yabe [9] gives

$$q = -\frac{\epsilon}{\sigma_e} \bar{E} \cdot \nabla \sigma_e, \tag{16}$$

which neglects the variation of the permittivity.)

Assuming that ϵ and σ_e are functions of temperature only, equation (15) gives

$$q = \bar{E} \cdot \nabla T \frac{d\epsilon}{dT} - \frac{\epsilon}{\sigma_e} \bar{E} \cdot \nabla T \frac{d\sigma_e}{dT} \tag{17}$$

in a thermal field.

In the case of a.c. fields of frequency f, the magnitude of the fluid charge relaxation time τ, where $\tau = \epsilon/\sigma_e$, determines whether free electric charge can build up in the fluid, which can then be acted upon by the electric field. In convective flows with free charge present, the EHD effect becomes important when τ is of the same order as, or less than, the time needed for the fluid to traverse the electric field [10].

If there is a spatial change of ϵ then the second term of equation (1) becomes important. The direction of this component depends on the direction of increase of ϵ. This term can be expanded as follows:

$$-\tfrac{1}{2} E^2 \nabla \epsilon = -\tfrac{1}{2} E^2 \left[\left(\frac{\partial \epsilon}{\partial T} \right)_\rho \nabla T + \left(\frac{\partial \epsilon}{\partial \rho} \right)_T \nabla \rho \right]. \tag{18}$$

For non-polar fluids the first term in the brackets is zero and the equation above reduces to

$$-\tfrac{1}{2} E^2 \nabla \epsilon = -\tfrac{1}{2} E^2 \left[\left(\frac{\partial \epsilon}{\partial \rho} \right)_T \nabla \rho \right], \tag{19}$$

which indicates that the resultant component force is towards the heated surface. The same can be said in the case of polar liquids, although the resulting equation is more complicated. For non-polar fluids the Clausius–Mossotti relationship:

$$\left[\frac{\partial \epsilon}{\partial \rho} \right]_T \rho = \frac{(\epsilon - \epsilon_0)(\epsilon - 2\epsilon_0)}{3}, \tag{20}$$

can be used to simplify the third term of equation (1) to

$$\tfrac{1}{2} \nabla \left[E^2 \left[\frac{\partial \epsilon}{\partial \rho} \right]_T \rho \right] = \tfrac{1}{2} \nabla \left[E^2 \frac{(\epsilon - \epsilon_0)(\epsilon - 2\epsilon_0)}{3} \right] \tag{21}$$

(see Yabe [9]). (A similar equation can be derived for polar fluids.) This term of the EHD force is a gradient and thus cannot cause any vorticity in the fluid and was usually neglected, possibly

for this reason. It has, however, a significant effect at the interface and in two-phase heat transfer [9].

In two phase heat transfer, namely boiling and condensation, EHD enhancement can be attributed to the following factors which can act individually or in combination:

(a) *Action at liquid/vapour interface*

The EHD force acts to destabilize the layer of condensate or vapour forming during condensation and peak nucleate and film boiling, respectively [7, 11, 12]. Film condensation can reverse to pseudodropwise condensation and film boiling to nucleate boiling. In general, the destabilization caused by the electric field results in the reduction of the thermal resistance at the heat transfer surface.

(b) *Action on vapour bubbles*

Pohl [6] suggested that the dielectrophoretic force can act on an insulating sphere of radius R and permittivity ϵ_2 in a surrounding medium of permittivity ϵ_1 producing a force F given by

$$\bar{F}_d = 2\pi R^3 \epsilon_1 [(\epsilon_2 - \epsilon_1)/(\epsilon_2 + 2\epsilon_1)] \nabla E^2. \tag{22}$$

If $\epsilon_2 < \epsilon_1$, which is the case of a vapour bubble in a liquid, i.e. in boiling, the bubble is attracted to regions of lower electric field strength. (If $\epsilon_2 > \epsilon_1$ the sphere is attracted to regions of higher electric field strength.) A common geometry studied is one of a coaxial cylindrical electrode system. The heat transfer surface is an inner cylinder at radius r_1 and at earth potential ($\phi_1 = 0$), see Fig. 1. The outer cylinder, radius r_2, is at high voltage ϕ_2. Assuming that such a system is two-dimensional, i.e. a long cylindrical system, the electric field E, at any radius r, is given by

$$E = -\frac{\phi_2}{r \ln\left(\frac{r_2}{r_1}\right)} \bar{r}, \tag{23}$$

where $\bar{r}$ is the unit radial vector (positive away from the axis) and

$$E^2 = \frac{1}{r^2}\left[\frac{\phi_2}{\ln\left(\frac{r_2}{r_1}\right)}\right]^2. \tag{24}$$

Then

$$\nabla E^2 = -\frac{2}{r^3}\left[\frac{\phi_2}{\ln\left(\frac{r_2}{r_1}\right)}\right]^2 \bar{r}. \tag{25}$$

Therefore, the force on the sphere (or a bubble assumed to remain spherical) is

$$\bar{F}_d = -4\pi \frac{R^3}{r^3} \frac{\epsilon_1(\epsilon_2 - \epsilon_1)}{(\epsilon_2 + 2\epsilon_1)}\left[\frac{\phi_2}{\ln\left(\frac{r_2}{r_1}\right)}\right]^2 \bar{r}. \tag{26}$$

In experiments with refrigerants the resulting electrodynamic force on the bubbles could be comparable or significantly higher than the gravitational force. In the experiments of Karayiannis

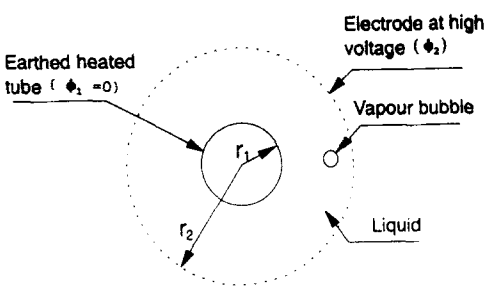

Fig. 1. Heated tube concentric with a cylindrical electrode.

et al. [13] with R114, the outer cylinder had a diameter of 38 mm and the inner, earthed heat transfer cylinder 19.1 mm. For 20 kV applied at the outer cylinder and dielectric constants of liquid and vapour refrigerant of 2.17 and 1.0 respectively, the resulting magnitude of the electrodynamic force on a bubble located at the heat transfer surface is

$$F_d = 5.13 \times 10^4 R^3.$$

The buoyancy force is given as

$$\bar{F}_b = \tfrac{4}{3}\pi R^3(\rho_1 - \rho_2)\bar{g}. \tag{27}$$

For a liquid and vapour density of 1441 and 7.74 kg/m^3 respectively, the force magnitude is

$$F_b = 5.89 \times 10^4 R^3,$$

which is comparable to the EHD force. In heat transfer from smaller diameter cylinders (or in the extreme, from wires) the EHD force can predominate, since it is proportional to $1/r^3$.

In the experiments of Winer [14], again with R114, the ratio r_2/r_1 was $50.8 \times 10^{-3}/5.5 \times 10^{-3}$. For 20 kV the resulting dielectrophoretic force on the bubble is

$$F_d = 19.7 \times 10^4 R^3;$$

this is approximately 3.3 times higher than the buoyancy force.

The acceleration of the bubble can cause agitation of the neighbouring boundary layer liquid and thus improve the heat transfer rates. However, the heat transfer rates can be greatly enhanced if the bubbles are made to adhere and move along the heat transfer surface. In cases where the tube outer surface is made of fins (low fin tubes), the local variation of the electric field and thus the local dielectrophoretic force can be different both in magnitude and direction than the force on a smooth surface. In the case of a low fin tube, the field is progressively weaker from the tip to the root of the fin. The dielectrophoretic force can then move the generated bubbles to the spacing between the fins. Columns of vapour can subsequently form which grow until the buoyancy forces overcome the EHD force [15].

If the charge relaxation time is far greater than the bubble detachment period, the bubbles are not affected by the electric field [16]. Differences in the charge relaxation time of R123 and R11 (0.89×10^{-3} and 1.3 s [16]) respectively could account, among others, for the higher enhancement ratio obtained for R123 in the experiments of Ohadi *et al.* [17]. It is therefore evident that the charge relaxation time of fluids can be a very important parameter both in single and two-phase heat transfer enhancement.

(c) *Change in contact angle and surface tension*

In the case of nucleate boiling, Rohsenow [18] has shown that the degree of superheat needed for bubble growth at a given bubble size depends directly on the surface tension of the liquid–vapour interface. Also, the contact angle, θ, is related to the surface tension by

$$\cos\theta = \frac{\sigma_{wl} - \sigma_{gw}}{\sigma_{lg}}, \tag{28}$$

where σ_{wl}, σ_{gw} and σ_{lg} are, respectively, the surface tensions at solid–liquid, vapour–solid and liquid–vapour interfaces [19]. Both θ and surface tension have been observed to vary with electric field strength [12, 20] and this would explain the initiation of ebullition by an electric field at reduced superheat.

3. SINGLE PHASE HEAT TRANSFER

The three major ways in which EHD can enhance single phase convective heat transfer are:

(a) by flow of "corona (or electric) wind",
(b) by electrophoresis, with or without charge injection,
(c) by dielectric phoretic forces,

but (d) EHD-induced flow can be used to improve normal convective effects.

(a) *Corona wind*

Accounts of this have varied from notes in technical journals, such as "developments to watch: a noiseless fan, with no moving parts" [21] to a full-scale design study for its application to a power station dry cooling system [22].

Generally, an array of sharp points or fine wires at high potential faces the surface to be cooled, at earth potential. Table 1 lists descriptions of arrangements for which numerical values of heat transfer enhancement are given and/or a practical application specified allowing for the fact that it is not always easy to distinguish between corona wind in tubular systems and similar geometries utilizing electrophoresis with charge injection.

Compared with other EHD enhancement phenomena, corona wind has relatively large energy consumption. For example, Holmes and Basham [22] show optimum performance for a 25 by 25 mm needle array at 51 mm from the heat transfer surface when corona power input is 30% of thermal throughput. Figure 2, from Moss and Grey [24], shows how an increase in the latter is related to the former. The "unit gradient" lines indicate "break even" to which the effect tends with increasing Reynolds number, *Re*.

(b) *Electrophoresis*

Electrophoresis would appear to give the best results but its effect depends critically upon the purity or otherwise of the heat transfer fluid, on whether it is polar or non-polar and upon whether or not charge is injected into it. Table 2 summarizes experimental work, most of it on annular arrangements, from fine wires to narrow ducts, some with, and some without, deliberate charge injection. Relatively large values of $q\bar{E}$ in equation (1) can be attained with modest energy expenditure. An ionization current i (A) from a source in a volume flow rate V (m^3/s) gives

$$q = \frac{i}{V} \quad (C/m^3) \tag{29}$$

and electrophoretic force

$$q\bar{E} = \frac{\bar{E}i}{V} \quad (N/m^3); \tag{30}$$

this can give rise to relatively large forces for little current consumption. For example, a gas flow of 670×10^{-6} m^3/s over an ionizing electrode fed with 50 μA gives a charge density of 0.075 C/m^3 which, acted on by an electric field of strength 1 MV/m causes a force of 75 kN/m^3 which is at least comparable with the pressure gradient causing flow (which depends on the nature of the duct cross-section). The generation of electric charge, which occurs when the electrical conductivity and/or permittivity have a spatial distribution, is described by equation (15).

Special mention should be made of two Russian contributions of the mid-1960s, by Baboi *et al.* [59] and Semenov *et al.* [60] which provide a link between electrophoretic and dielectrophoretic effects as well as, in ref. [59], with corona wind and between single- and two-phase heat transfer effects. They reviewed earlier work and reported their own natural convection experiments with air (70 μm dia. wire along axis of 17 mm dia. tube) and with transformer and castor oils (70 μm dia. wire 10 mm below and parallel to 4 mm dia. cylindrical electrode). In these, with air, a.c. stress gave α_E/α_0 increasing with E to a maximum (3.2 with wire temperature 52°C at 3.5 MV/m) then decreased, even causing inhibition, the maxima increasing and shifting to higher E with increasing temperature. By contrast, the oils gave unequivocal improvement but, whereas σ_E/σ_0 for castor oil increased continuously with wire temperature, for transformer oil it peaked and, between 208 and 375°C, decreased from 5.8 to 1.9 at $E = 39$ MV/m. Below 98°C, the curves are concave upwards, whereas with d.c. stress they tend to saturate, intersecting at $\alpha_E/\alpha_0 = 3.4$ and $E = 28.5$ MV/m, clearly showing that dielectrophoresis can give greater enhancement than electrophoresis.

(c) *Dielectrophoresis*

Dielectrophoretic enhancement was the first to be reported (e.g. by Senftleben [61], Senftleben and Braun [62]) and, although less effective than (a) or (b), is the simplest to compute [63] and correlate. It can assist the cooling of high voltage apparatus [64]. Table 3 reviews reported experimental work that can be classified under this heading.

(d) *EHD-induced flow*

Electrophoretic pumps can be classified as "induction" or "ion drag". The operation of the former depends on the electrical conductivity of the working fluid providing dissociated positive and negative ions, which are acted upon by the travelling electrostatic field. This field is set up by interleaved electrodes fed in pairs from a high voltage three-phase supply. If the free charges follow the apparent motion of this field, imparting their motion to the adjacent fluid, the pump is said to be an "attraction" one. Its action is analogous to magnetic linear motion in that the fluid velocity cannot exceed that of the travelling field. The simplest way of creating the free charges is by means of a temperature—and hence electrical conductivity—gradient [see equation (16)] perpendicular to the pumping direction. When heat is transferred from the fluid to the duct walls, the resulting distribution of conductivity, and hence of charges, favours the attraction mode, but if the heat transfer is in the opposite direction, the charge distribution gives flow against the field and the mode of operation is "repulsion" [71]. In either case, the net electrical charge in the fluid is zero, whereas in the ion drag pump charge is injected and then propelled by the electric field between injector and collector electrodes [72].

All EHD pumps are characterized by low efficiencies; the highest reported in the work reviewed here is 10%. However, low efficiency is considered offset by freedom from moving parts.

As has been shown, most recently by Sato *et al.* [73], dielectrophoretic pumping action in an isothermal liquid can also provide convective flow to improve heat transfer conveniently and efficiently. However, the work of Sayed-Yagoobi and collaborators [71, 72, 74–79] has concentrated on induction ion drag pumps and therefore depends on electrophoresis. Nevertheless, to state, as does ref. [77], that "the dielectric fluid being pumped must contain free charges" cannot be accepted. Whether electrophoretic or dielectrophoretic, EHD pumping is possible and recent experimental work is summarized in Table 4.

4. TWO-PHASE HEAT TRANSFER

(a) *Condensation*

Publications on the EHD enhancement of condensation began appearing in 1965 with the work of Velkoff and Miller [80] and Choi and Reynolds [81] using R113. This literature is reviewed in Table 5. Several themes can be discerned. First, condensation has been studied on surfaces that are flat or curved, horizontal or vertical. In all cases, the disposal of the condensate, once formed, can be a problem. On a vertical surface, as the condensate film thickens with increasing distance downwards, heat transfer coefficients reduce. In banks of horizontal tubes, the same effect results from condensate dripping from those above. Smirnov and Lukanov [95] report a $>60\%$ reduction in heat transfer coefficient between rows numbers one and five for R11 condensing on a bundle of low fin tubes.

As shown in Fig. 3, even the best EHD-assisted performance falls short of that given by using a single low fin profile tube. EHD has little effect on low fin tube condensation as it and the Grigorig effect act in opposition. However, in addition to destabilizing the condensate film, EHD can strip condensate off the surface and overcome the effects described in the previous paragraph. Figure 4 shows that EHD enhancement of R114 condensing on a smooth, 506 mm long, 19.1 mm o.d. brass tube with vapour to tube-wall mean temperature difference of 25 K is of much the same magnitude whether the tube is horizontal or vertical. Values of α'_E/α_0 from the measurements of Cooper [96] are given as a function of voltage applied to a 38 mm i.d. cylindrical copper gauze electrode surrounding the tube. (Measured mean heat transfer coefficients α_E at electric field strength E have been corrected to primed values α'_E taking into account the increase due solely to reduced ΔT [89].) The work described above relied on thinning the condensate film. Heat transfer enhancement ratios (up to 4.5) were obtained using an electrode geometry that strips the condensate from the surface [91], see Section 6. Higher heat transfer enhancement ratios—up to 20—were also reported in refs [11, 83, 85]. Heat transfer coefficients are considerably reduced in the presence of a non-condensable gas. Bologa *et al.* [92] reported that the damaging effect of the gas can be nullified by the application of an electric field.

Table 1. Review of published experimental work on augmented single phase heat transfer using corona wind

Author(s)	Heat transfer fluid(s)	System	$\left(\frac{\alpha_E}{\alpha_0}\right)_{max}$	Notes
Holmes and Basham [22]	Air	Electrically heated vertical copper plate, plane or finned, facing array of needle electrodes.	>6 (for 25 mm by 75 mm needle array at 51 mm spacing).	Compared with effect of air jets normal and parallel to surface (corona wind intermediate between the two). Better results with finned plate. Conceptual design of 2GW system.
Velkoff [23]	Air, oxygen, nitrogen	Horizontal isothermal heated tube, 31.75 mm i.d., with axial stainless steel corona wire, 127 μm dia., starting lengths 6, 13 and 24 dia.	2 (at Re = 3000 wire + ve. Little difference between i_c = 0.5 and 1.0 mA).	In laminar regime, increased friction factor expressed as increase of effective viscosity (doubled at i_c = 1 mA, greater with − ve wire).
Moss and Grey [24]	Nitrogen	Horizontal isothermal heated tube, 305 mm long, 25.4 mm i.d. No details of axial wire.	1.35 (at Re = 1200, + ve wire).	Part of a more general programme of EHD research. Negative wire gave inhibition.
Grosu and Bologa [25]	Air, argon, carbon dioxide, helium	Heated 0.2 mm dia. nickel wire in coaxial high voltage cylinder, 37 mm dia.	~3 (air at 1 atm and helium at 21 atm). 2.5 (argon at 1.4 atm). 5 (carbon dioxide at 1 atm).	Detailed analysis given for this geometry. Effect increased with pressure at i_c constant.
Robinson [26]	Air	Heated platinum wire, 508 μm dia., at high voltage, along axis of vertical steel tube, 53.2 mm i.d., with and without forced convective cooling.	4.2 (with wire 260°C and natural convection).	Corona discharge at heat transfer surface itself.
McDermott [27]	Air	Various arrangements for zero-field temperatures 130–590°C. High voltage applied with various sharp probes.	~4	Schlieren observation shows mechanism. Power consumed 3 W compared with 14 W by fan.
Mizushima, Ueda, Matsumoto and Waga [28]	Air	Vertical copper tubes, with 42 mm i.d. PVC water jacket, cooling hot air passing downwards with axial nickel wire 300 μm o.d. Tubes: 6.4 mm i.d., 520 mm long and 15 mm i.d., 980 mm long.	4 (at Re = 700). 2.5 (at Re = 2000).	Little effect at Re > 4000.
Windischmann [29]	Air	Point above plane.	2 (locally)	Effect decreased for temp. >200 K.
Yamaga and Jido [30]	Air	Corona wind focused by shaped intermediate potential ring on to (earthed) cooled object (cutting tool).	—	Performance assessed by tool wear reduction.
Kibler and Carter [31]	Air	10 mm dia. tubular assembly incorporating point at 5 kV spaced 5 mm from (earthed) grid.	—	To be used in arrays.
Yabe, Mori and Hijikata [32]	Nitrogen at 10^5 Pa	40 μm dia. wire, 120 mm long, at 8.3 kV, 20 mm below 100 mm by 100 mm, flat, heated copper plate.	12 (locally)	Detailed experimental and theoretical analysis in ref. [33].
Velkoff and Godfrey [34]	Air	152 μm dia. wires, spaced 12.7 mm parallel to, and 6 mm from, vertical electrically heated, 483 mm by 251 mm, plate.	−3.5	Improved heat transfer if stream velocity $\not>$ 10 times free convection velocity.

Tada, Takimoto and Hayashi [35]	Air	Horizontal parallel uniformly heated plates, 650 mm long, 225 mm wide, spaced 30 mm apart with 200 μm dia. midplane ionizing wires, spaced 40 mm at 0–12 kV and either: (1) parallel to flow or (2) transverse to flow. Also: (3) single ionizing wire followed by mid-plane electrode (with gas–solid suspensions).	(1) 3.7 (2) 1.8 (3) 2.5	$600 < Re < 8000$. Flow patterns visualized and computed.
Nelson, Ohadi, Zia and Whipple [36]	Air	Horizontal tube, 1590 mm entrance, 1020 mm test and 410 mm exit sections, axial 250 μm dia. ionizing wire. (Also, dual wire arrangement giving slightly greater effect.)	3.6	Peaks at $2000 < Re < 3000$ and positive polarity. Pressure measurements made. Correlations use non-dimensional variable, *Ne* (Section 5).

Secondly, from the earliest work, relationships have been suggested for correlating the results of different experiments. This subject is dealt with in detail later.

(b) *Boiling*

By contrast with condensation, boiling appears to have benefited from EHD since 1916, when a threefold increase in water evaporation rate was claimed by Chubb [97]. However, the present era of such EHD usage began with the work of Bochirol *et al.* [98] and Bonjour *et al.* [99], published in 1960 and 1962, closely followed by Watson [67], Choi [100], Jalaluddin and Sinha [101] and Markels and Durfee [20, 102], all except ref. [102] for pool boiling. The work used a wide variety of fluids and, with subsequent work, is reviewed in Table 6.

To define terms used in Table 6, Fig. 5 shows a typical boiling characteristic curve in terms of thermal flux per unit area, $\dot{q}$, vs superheat, ΔT. Starting from $\Delta T = 0$, the heat transfer process proceeds along curve AB, by natural or forced convection, to C, where ΔT is sufficient to initiate nucleate ebullition, thus giving greatly increased $\dot{q}$ (at D); $\dot{q}$ then continues to increase with ΔT until (at E) it reaches a value $\dot{q}_c$ known as peak nucleate boiling, critical or maximum, heat flux density where the coalescence of the bubbles forming at the heat transfer surface into an unstable film begins to impede energy transfer. This decreases $\dot{q}$ from E to F through a transition region of partial film boiling until, at F, a minimum film boiling condition ($\dot{q}_{min}$) given by a stable, blanketing, vapour film. Increasing ΔT then gives stable film boiling, with increasing $\dot{q}$, beyond F. If, from beyond D, ΔT is decreased, nucleate boiling continues along DB′ towards A, giving "boiling hysteresis".

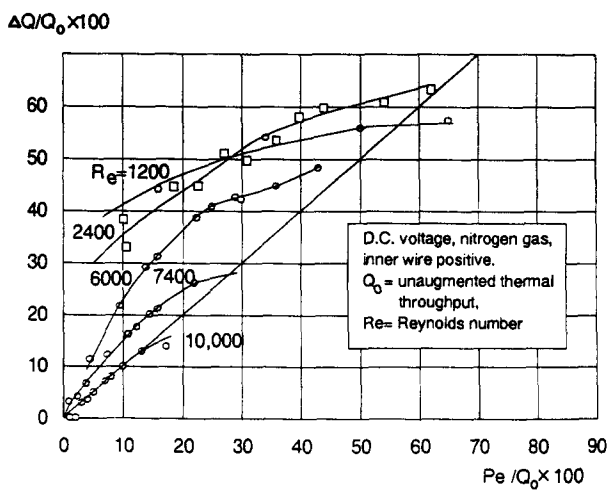

Fig. 2. Increase ΔQ in total thermal throughput as a function of electrical power input P_e [24].

Table 2. Review of published experimental work on augmented single-phase heat transfer due to electrophoresis

Author(s)	Heat transfer fluid(s)	D_i, D_0, L (mm)	E_{max} (MV/m)	$\left(\frac{\alpha_E}{\alpha_0}\right)_{max}$	Notes
Annular systems					
Schmidt and Leidenfrost [37, 38]	Transformer oil	10, 18, 500 (horizontal)	6.9	4	Forced convection α values overall, water to oil. (Oil side values estimated in [39].) (Relatively small) pressure drop change measured.
Allen [39]	Transformer oil to BS148	0.025, 22, — (vertical)	8.4	~ 1.2	Steady d.c. stress gave inhibition which changed transiently to enhancement when polarity reversed and permanently when mixed with a.c. Results of [37, 38] analyzed assuming mixed a.c./d.c. stress.
Mascarenhas, Mascarenhas, Ferreira De Souza and Rabello [40]	Fatty acids: stearic oleic palmitic	(vertical)	—	1.3 1.4 1.4	Effect deduced from heating curves. A.c. much less effect than d.c. Joulean heat shown to be negligible.
Senftleben and Schnabel [41]	Cyclohexane	0.05, 10, 20 (horizontal)	2.2		Investigates and explains d.c. inhibition due to space charge at low E and ΔT in good insulators.
Care and Swan [42]	Transformer oil	0.025, 25, — (horizontal)	35	—	Followed up [39] by investigating: (1) boundaries between inhibition and enhancement at much higher d.c. E, finding oscillatory regime (2) transient due to polarity change as function of pre-stressing and relaxation times.
Porter and Poulter [43]	Transformer oil	1.58, 31.8, 2800 (horizontal)	6.7	1.9	Forced convection. Negative voltage gave greater, 50 Hz zero, effect. Much greater pressure drop needed for same heat transfer increase without elect. field.
Newton and Allen [44]	Transformer oil	344, 364, 500 (vertical-insulated and uninsulated-heat transfer surfaces)	2	2	Forced convection. No consistent difference between positive and negative polarity but uninsulated heat transfer surface shows somewhat greater improvement.
Poulter and Miller [45]	Avtur, hexane (injection strength estimated 0.7, 0.05)	3.2/1.6, 12.4, 600 (horizontal)	18.3	~ 20	Forced convection. Defines injection strength parameter as $q'/\epsilon E$, and correlation parameter as $\phi\sqrt{(\rho/\mu}$.
Fernandez and Poulter [46]	Transformer oil	1.59, 25.4, 1000	6.8	6	Forced convection. Greater improvement using negative polarity.
		1.59, 19.1, 1000 (horizontal)	7.6	23	Pressure drop increased by up to 66%. Current drawn $\gtrsim 10\,\mu$A. Radial flow pattern observed.
Gap between horizontal plates (Heat transfer downwards)					
		Dimensions			
Mascarenhas [47]	Oleic acid	2 mm thick layer.	1.25	1.36	Used steady state thermal conductivity apparatus. Joulean heat shown to be negligible.

Borbulya, Kojuhar and Bologa [48]	Transformer oil	(a) Disks 70 mm dia. (b) Cylinders, 34 mm dia. by 100 mm long (spacing unspecified).	1.5	3	
Gross and Porter [49]	Transformer oil	50 mm dia. cell.	0.3	—	Study of convection patterns due to d.c. fields. No a.c. effect.
Turnbull [10]	Corn oil	102 mm by 76 mm aluminium plates separated 25 mm.	~3	10	Part of an extensive study into the instability due to an electric field.
	castor oil		~3	6	
Rectangular duct (forced convection)					
Porter and Smith [50]	Transformer oil	Horizontal, 180 mm by 17 mm section, 1230 mm long, upper wall heated.	~1	1.9 at $Re = 95$, $\dot{q} = 9.1$ kW/m^2.	(Relatively small) friction factor increases measured. Effect on heat transfer coefficient decreased with Re and increased with heat flux.
Fujino, Yokoyama and Mori [51]	R113	Vertical, 120 mm by 2 mm section, 200 mm high, one wall heated.	1.5	8	Mechanism of effect explored by shadowgraphs.
Ishiguro, Nagata, Yabe and Nariai [52]	"Furonsorubu AE", (96% R113, 4% ethanol)	Horizontal, 150 mm by 20 mm section, test section, 600 mm follows 1000 mm entry with 14 off 300 μm dia. stainless steel wires, 20 mm apart, 5 mm from wall, both walls heated.	—	20 at $Re = 1470$, 3 at $Re = 27300$, wires at 10 kV.	Heat transfer and pressure drop increase factors decreased with Re. Heat transfer increases greater than pressure drop increases.
Nuclear reactor applications					
Stach [53]	Air	Reactor cooling channel: no details given.		1.2	For average velocity ($\bar{v}$) range 4–23 m/s, reactor power (V_R) 200–2000 kW and voltage (ϕ) 1–3 kV, Nu increased linearly with $V_R\phi/\bar{v}^2$. Flow of partially ionized gas analyzed (in two dimensions).
Berger and Derian [54]	(1) (a) air, (b) CO_2 (120–190°C) at low (up to 2 atm) pressures.	Annuli (1) 41 mm o.d., 28 mm i.d., 485 mm long.	0.56	1.5	Up to 50% enhancement and 8% inhibition depending on pressure, polarity and (HV power)/(gas velocity)$^{2.5}$.
	(2) CO_2 (35–75°C) at high (up to 30 atm) pressures.	(2) 42 mm o.d., 28 mm i.d., 500 mm long.	5.28		
Berger and Derian [55]	More experimental details of ref. [54] above				
Miscellaneous systems					
Coulson and Porter [56]	Liquid paraffin	Heated tubes, 3.2, 4.7, 6.4, 9.5 and 12.7 mm dia., 152 mm long, parallel to 1 mm dia. HV electrode.	—	1.8	Results for d.c. (polarity not specified), effects of a.c. "much less".
Schnurmann and Lardge [57]	Perfluoromethylcyclohexane (non-polar)	127 μm dia., 260 mm long, heated platinum wire parallel to, 27.7, 25.4 and 50.8 mm from, 254 mm by 50.8 mm plate electrode.	~60	2.4 both +ve and −ve.	Part of study including boiling. Clarified importance of electrical nature of fluid. α_E/α_0 graphs suspect as they converge at origin.
	20% isopropyl alcohol in n-heptane, (polar)		~48	8.7 electrode positive.	
	pure n-heptane (polar)		~60	4.4 electrode negative.	
Cooper and Allen [58]	Transformer oil to BS148	Facsimile shell/tube heat exchanger with array of three earthed, water-heated tubes, 12.6 mm o.d., spaced 16.6 mm vertically, between electrodes with 4 mm clearance.	3.6	2.3	Positive electrode has much less effect. Effect decreases with Re, very sensitive to contamination by air and to ΔT. Circumstances giving inhibition found but turned to enhancement with low frequency alternating polarity.

Table 3. Review of published experimental work on augmented single-phase heat transfer due to dielectrophoresis

Author(s)	Heat transfer fluid(s)	D_i, D_0, L	E_{max} MV/m	$\left(\frac{\alpha_E}{\alpha_0}\right)_{max}$	Notes
Annular systems					
Senftleben and Braun [62]	Argon, oxygen (non-polar), carbon monoxide (slightly polar), ethyl chloride (polar).	30 or 50 μm, 5–45 mm, 70 mm, horizontal.	10.7	1.5 (ethyl chloride).	Cylinder in cryostat or oil bath at temp. between 90 and 400 K. Pressure 0.116–0.986 bar. A.c. and d.c. used, no polarity effect. Experimental data given in full.
Ahsmann and Kronig [65]	Toluene, *n*-heptane (pure and commercial) carbon tetra-chloride, ammonia gas.	20 μm, 40 mm, 70 mm, horizontal.	9.2	1.5 (carbon tetra-chloride).	Cylinder in melting ice. High voltage 40 Hz square wave and d.c.
De Haan [66]	*n*-heptane, toluene.	22, 55 and 99.5 μm, 40 mm, 160 mm, horizontal.	5.0	1.3 (*n*-heptane).	Cylinder in thermostat, 40–80 C. Greater variation of $\bar{T}$ and D_i than [65]. High voltage as [65].
Watson [67]	*n*-hexane.	100 μm, 30 mm, 100 mm.	24.5	2.6	D.c. stress, no polarity effect.
Vertical ducts					
Weber and Halsey [68]	"Transil" insulating oil	Rogowski (uniform field) electrodes, 25.4 mm dia., one heated, spaced 5.1–20.3 mm.	9.6	3.6	60 Hz stress.
Savkar [69]	Light mineral insulating oil	Duct 762 mm long, 305 mm wide, up to 12.7 mm thick (with equal length entry section).	7.3	2.2	60 Hz stress. One or both sides heated. Longitudinal roll cells predicted from analytical solution of governing equations, including EHD forces, confirmed experimentally. α_E/α_0 decreases with *Re*.
Newton and Allen [44]	Transformer oil to BS148	Facsimile transformer winding ducts, 12.7 mm by 57 mm by 339 mm long, 6.3 mm by 28 mm by 267 mm long (with entry length sections).	6	1.25	50 Hz stress.
Wang, Collins and Allen [63]	Transformer oil to BS148	As ref. [44].	6	1.25	Governing equations solved numerically to include EHD forces confirmed by experiments of ref. [44].
Miscellaneous system					
Oliver [70]	Sulphur hexafluoride	—	8	—	Gas pressure 10 bar. Conductor dia. 33 mm. No effect observed.

EHD eliminates the $\dot{q}$ decrease between E and G and, in addition, increases $\dot{q}_c$. These phenomena have received very much more attention than EHD's other action, namely the initiation of nucleate boiling at smaller ΔT and hence the virtual elimination of the hysteresis portion (ABCDB'A) of the characteristic, e.g. by applying volts at ΔT values between b and c. This initiation process has been reported only by Karayiannis *et al.* [13], Jalaluddin and Sinha [101], Basu [104] and Allen and Cooper [15] who have also made a video record of it [117]. In this, observation is made of a tube, immersed in R114. Hot water passes along the tube, losing heat to the refrigerant. Thus, near the inlet, the tube surface gives sufficient superheat for bubbles to evolve at a well-defined set

Table 4. Review of recently published experimental work on EHD pumping

Author(s)	Fluid(s)	System	Flow rate	Notes
Induction (attraction)				
Seyed-Yagoobi, Chato, Crowley and Krein [74]	Sun No. 4 oil with added Shell ASA-3 antistatic additive to vary σ_e.	Total loop length 5.2 m, vertical limbs 2.1 m, 16 mm i.d., 3-phase electrode system formed by alternate metal and glass rings forming tube ~1 m long. 30 kV 3-phase supply, 0–100 Hz, reversible. Natural convection generated by heating or cooling.	50 mm/s (4× natural convection rate) at optimum frequency (~5 Hz) and oil σ_e.	Heated section of return limb gave natural convection (forward) flow from top to bottom of pump. Some flow detected without heating or cooling.
Bohinsky and Seyed-Yagoobi [75]	4 synthetic petroleum fluids, 4 petroleum oils, 1 polyol ester, 1 fluorinated fluid, 1 aromatic hydrocarbon, 1 silicone fluid, some with added over-based calcium sulphonate to vary σ_e.	Total (vertical limb) loop length 2.2 m, 50 mm i.d., 430 mm long 3-phase electrode system formed by 18 gauge copper wire in grooves. 12 kV 3-phase supply, 0–13 Hz, sine, square or triangular waveform.	Maximum 385 mm/s obtained with doped aromatic hydrocarbon (*n*-hexane) at 9 Hz.	Higher than synchronous velocities observed but not explained.
Ion-drag				
Castañeda and Seyed-Yagoobi [78]	R11	Total (horizontal) loop length 2.68 m, 50 mm i.d., pumping section 360 mm long. 13 electrode pairs, 8 mm apart, spaced 15 mm, formed by 20 gauge tin-copper wire in grooves, using no sharp points. 50 kV supply.	Maximum 240 mm/s with all electrodes energized at 28.5 kV	Current consumption and velocity linear functions of number of energized electrodes.
Bryan and Seyed-Yagoobi [77]	3 synthetic petroleum fluids, 4 petroleum oils, 1 fluorinated fluid, 1 aromatic hydrocarbon, 1 silicone fluid.	Total (vertical) loop length 1.92 m, 70 mm i.d., pumping section 330 mm long. 10 electrode pairs, 10 mm apart, aluminium electrodes spaced 5 mm, upper (emitter) electrode fitted with 90 stainless steel needles, pointing at collector electrode. 50 kV supply.	220 mm/s obtained with undoped synthetic petroleum fluid (dodecyl-benzine) at 20 kV.	Efficiency ($\not>$5.5%) increased with charge relaxation time.
Bryan and Seyed-Yagoobi [79]	Dodecylbenzine	Two pump sections: (a) as ref. [77] but with total loop length 1.86 m. (b) with one electrode pair only, giving loop length 1.33 m and also having modified collector electrode (with stainless steel wire web extending 6 mm radially inward). 50 kV supply.	334 mm/s with undoped fluid and 10 electrode pairs at 25 kV.	Increasing σ_e reduced flow rate. Higher efficiency and slightly higher velocity with plain collector electrode.
Dielectrophoretic				
Sato, Yabe and Taketani [73]	"Furonsorubu AE" (96% R113, 4% ethanol), R113, R123.	24 mm square, about 160 mm long, horizontal pump section containing 61 mm long, 20 mm square hollow high voltage electrode adjacent to various (toroidal, rod, spherical) earthed electrodes.	143 mm/s with toroidal electrode at 20 kV.	Effect of flow on convective heat transfer estimated. Other (less effective) electrode arrangements tested.

of sites. However, towards the outlet, ΔT is only sufficient to give convective heat transfer and thus a well defined "front" is seen between boiling and non-boiling regions. On application of electrode voltages greater than about 8 kV there is immediate—and more vigorous—ebullition everywhere on the tube surface. In at least one case (Baboi *et al.* [111]), the phenomenon was deliberately

Table 5. Review of published experimental work on EHD augmented condensation heat transfer

Author(s)	Heat transfer fluid(s)	System	$\left(\frac{\alpha_E}{\alpha_0}\right)_{max}$	Notes
Velkoff and Miller [80]	R113	Vertical cooled cooper plate, 152 mm high, 229 mm wide, facing: (1) 102 μm dia. horizontal wire (2) Mesh screens (3) Aluminium plate.	~1.4 ~3 ~1.7	3, 4, 5, 6
Choi and Reynolds [81]	R113	Vertical stainless steel tube, 1346 mm long, 23.8 mm i.d., cooled on outside and coaxial with inner electrodes 6.3, 12.7 and 19.1 mm o.d..	2	1, 2, 3
Choi [82]		As for Choi and Reynolds [81].		
Holmes and Chapman [83]	R114	Flat silver-plated copper cooled and electrode plates (each 152 mm—horizontal—by 38 mm—sloping) at different angles to give variable wedge shaped enclosure.	Up to times 10 (overall).	6, 7
Seth and Lee [84]	R113	Horizontal copper water tube with coaxial outer electrode.	1.6	5, 8
Bologa and Didkovskiy [11]	R113, hexane, diethyl ether	Vertical copper plate, 220 mm by 120 mm, spaced 7 mm from parallel (plain or horizontally slotted) electrode.	10 (for R113 & hexane) 20 (for ether).	2
Didkovskii and Bologa [85]	As for ref. [11].	As for ref. [11] together with vertical annulus, cooled tube 300 mm high 21 mm o.d., electrode tube 35 mm i.d.	As for ref. [11].	2, 5, 6
Didkovsky and Bologa [86]		As for Bologa and Didkovskiy [11].		2, 3, 7, 9
Smirnov and Lunev [87]	R113, diethylether	Vertical annulus, cooled outer jacket, 215 mm high 30 mm i.d., around central electrode with smooth, screw-threaded or perforated surface, gaps 2.5 to 4 mm.	3.6	2, 3, 6, 7
Yabe, Kikuchi, Taketani, Mori and Hijikata [88]	(a) Water	Needle electrode above liquid surface.		10
	(b) R113	Cooled brass plate, 600 mm high, 100 mm wide with shaped copper wire electrode systems.	2.24	3, 11
Cooper and Allen [89]	R12 and R114	Single cooled horizontal tubes 514 mm long with smooth (19.1 mm o.d.) and low fin (19.0 mm o.d.) surfaces. Electrode system: (1) concentric copper gauze (38 mm i.d.) (also vertical with R114) (2) Parallel brass plates with auxiliary 6.25 mm o.d. rod (to simulate (1)).	2.9	3, 5, 7, 12, 13
Trommelmans and Berghmans [90]	R11, R113 and R114	Horizontal smooth copper cooled tube 1100 mm long, 18 mm o.d., concentric with copper wire spiral electrode, 38 mm i.d.	1.1	3, 14

Yabe, Taketani Kikuchi, Mori and Maki [91]	(a) Silicone oil	Thin liquid film on and between electrically conducting glass sheets.		3, 5
	(b) R113	Vertical smooth brass cooled tube 540 mm high, 18 mm o.d. with copper helical (condensate removal) wire, 0.5 mm o.d. and curved (stress applying) plate electrodes, 21.2 mm o.d.	4.5	12
Bologa, Savin and Didkovsky [92]	R113–helium R113–air R113–carbon dioxide Hexane–air	Flat plate 200 mm high 120 mm wide with parallel plate electrode (having slits) or wire electrode (0.18 mm wires spaced 5 mm apart).	1.8 2.6 3.0 5.0	2, 3, 4, 5, 8
Damianidis Collins, Karayiannis and Allen [93]	R114	Horizontal bundle of nine smooth surface tubes, 19.1 mm o.d., 360 mm long. Perforated plate and rod electrode.	1.08	3
Yamashita, Kumagai, Sekita, Yabe, Taketani, and Kikuchi [94]	R114, *n*-perfluorohexane	Verticle bundle of 102 smooth surface stainless steel tubes, 19.05 mm o.d. with combined lattice/helical wire electrode system. Condensing temp.: 90 °C (R114) and 150 °C (*n*-perfluorohexane).	6 4	2, 3, 5, 15, 16

Notes:
(1) Analysis in terms of perturbation wavelength.
(2) Results correlated.
(3) D.c. electric field.
(4) Corona discharge gave electrophoresis.
(5) Condensate film perturbation observed.
(6) Condensate spraying observed.
(7) A.c. electric field.
(8) Inhibiting effect of non-condensable gas partly neutralized by EHD.
(9) Condensate film thickness measured.
(10) Gas–liquid interface stability studied theoretically and experimentally.
(11) Improved heat transfer due to condensate removal by electrodes measured.
(12) α_E Values corrected for reduced ΔT.
(13) EHD effect with low fin tube $< 10\%$.
(14) Effect of EHD on shape of pendant condensate droplets discussed.
(15) Tube length effect studied.
(16) Electrode power consumption increased by oil contamination.

avoided by reducing the thermal loading to the experimental value required (i.e. along EDB′ in Fig. 5) "so that most of the vapour-formation centres were active". Also, as remarked by Markels and Durfee [20], "It appears likely however that differences exist between voltage effects when a relatively large diameter heat transfer surface is used and when the boiling takes place on a thin wire". A fine wire fed by a constant electric current cannot instantaneously provide the additional thermal energy demanded by suddenly promoted ebullition. The energy could only come from a considerable decrease in temperature, and hence in ΔT, thus suppressing ebullition before it became established. By contrast, the more usual industrial case of a source heated by fluid flow maintains a much more nearly constant temperature, as can a high thermal capacity source (see Table 6 notes).

EHD boiling heat transfer investigations included tests with a variety of tubular surfaces including smooth, low fin and enhanced surfaces such as Thermoexel. It was found that the nucleate boiling heat transfer enhancement obtained on a smooth tube was very moderate compared with the low fin and the Thermoexel tubes. The most recent work in this area (based on data from refs [13, 96, 118]) is summarized in Fig. 6 on a "tube rating" (kW per metre of tube vs ΔT) basis which, for a given tube diameter, governs heat exchanger design.

Although, as shown in Table 6, a variety of geometric configurations was examined, only recently have researchers concentrated their efforts on tube bundles in heat exchangers like the shell and tube. Damianidis *et al.* [116] reported experiments on nine tube bundles consisting of either smooth or low fin tubes. The working fluid was R114. In the case of the low fin tube bundle, the

Table 6. Review of published experimental work on EHD augmented pool boiling heat transfer

Author(s)	Heat transfer fluid(s)	Heated surface diameter (mm)	$\left(\frac{\dot{q}_{c,F}}{\dot{q}_{c,0}}\right)_{max}$	$\left(\frac{\alpha_F}{\alpha_0}\right)_{max}$	Notes
Coaxial cylindrical systems					
Bochirol, Bonjour and Weil [98]	Benzene, hexane, trichlorethylene, toluene, ethyl ether, liquid nitrogen	0.2		2.7 (trichlorethylene and ethyl ether)	3,6
	Pure water, methyl ethyl ketone, acetone, methyl alcohol	0.1		6 (methyl alcohol)	
Bonjour, Verdier and Weil [99]		As for Bochirol, Bonjour and Weil [98]			
Watson [67]	*n*-hexane	0.1		2.6	2, 6
Choi [100]	R113	0.254 or 0.508	>2		1, 4, 6
Markels and Durfee [20]	Isopropanol, distilled water	9.525	6 >1.4		2, 5, 7
Winer [14]	R114	5.57	1.6		1, 2, 6
Lovenguth and Hanesian [103]	R21, R113, carbon tetrachloride, chloroform	0.51	2.9		1, 2, 6
Basu [104]	Carbon tetrachloride	0.040			2, 3, 6, 8
Jones and Schaeffer [105]	R113	0.127 or 0.406			1, 4, 6
Jones and Hallock [106]	R113, R113/methanol	0.812, 1.15 or 1.83			4, 5, 6
Zheltukhin, Solomatnikov, Mikhaylov and Usmanov [107]	Acetone, benzene, *n*-diethyl ether	5.0 to 6.5		1.82 (acetone)	5, 6
Allen and Cooper [15]	R114	18.6 low fin o.d.		up to 60	2, 7, 8
Kawahira, Kubo and Yokoyama [108]	R11	22.4		4	2, 3, 6, 8 10, 11
Karayiannis, Collins and Allen [13]	R114	19.1		4	2, 7, 8
Ohadi, Papar, Ng, Faani and Radermacher [17]	R123, R123/oil R11, R11/oil	12.7 o.d.		5.5 (R123) 1.7 (R11)	11
Parallel plate systems		*Electrode gap (mm)*			
Olinger and Colver [12]	Deionized water	6.35 or 25.4			2, 3, 6, 9, 10
Blachowicz, Brooks and Tan [109]	Benzene	5.0 to 20.0		2	3, 7, 9
Kawahira Kubo and Yokoyama [108]	R11	3.0		4.4	2, 3, 6, 10 11
Other systems		*System(s)*			
Jalaluddin and Sinha [101]	Methanol, isopropanol, methyl ethyl ketone, benzene	Heated sphere and plane electrode.			2, 3, 6, 8, 9
Asch [110]	R113	Heated wire (0.356 mm dia.) between 25.4 mm dia. discs spaced 25.4 mm or (asymmetrically) 12.7 mm dia. spheres with 60.3 mm gap.	6		2, 3, 6, 11
Baboi, Bologa and Klyukanov [111]	Benzene, toluene, liquid argon	Heated wires 0.05, 0.07 0.10 and 0.50 mm dia. parallel to 6.0 mm dia. cylindrical electrode.			1, 2, 3, 6, 11

Zhorzholiani and Shekriladze [112]	Acteone, benzene *n*-pentane	Heated horizontal tubes, 6.0 and 8.0 mm dia., parallel to plane electrode. Vertical semi-cylindrical heated channel facing plane electrode.	3 (acetone)		1, 2, 3, 6, 12
Rutkowski [113]	Liquid nitrogen	Heated horizontal wire, 0.10 mm dia., parallel to 3.0 mm cylindrical electrode.			3, 6
Yabe and Maki [114]	R113/ethanol ("Furonsuburu AE")	Heated plane beneath toroidal EHD "pump" electrode.	2.1		2, 7, 8, 13
Schnurmann and Lardge [57]	*n*-heptane, 20% solution of isopropyl alcohol in *n*-heptane, perfluoromethylcyclohexane	Heated earthed wire 0.127 mm dia. and 260.0 mm long electrode between two plates 254.0 × 508.0 mm one earthed and one at high potential.		~7 ~7 ~2	2, 6, 11
Tube bundles					
Damianidis, Karayiannis, Al-Dadah, James, Collins and Allen [115]	R114	Low fin tubes, dia. 19.05 mm, fin pitch 0.7 mm. Perforated plate and rod electrode.		2.5	2, 7, 8, 11
Ogata, Iwafuji, Shimada and Yamazaki [16]	R123	5-tube smooth tube bundle, 22 mm dia. 0.5 m long. Steel rod electrodes 6 mm dia. 3 mm from tubes.		7	2, 6
		50-tube smooth tube bundle, 22 mm dia. 0.5 m long. 12 electrode wires 3 mm from tubes.		7	2, 6
		80-tube smooth tube bundle. 22 mm dia. 2 m long. Steel rod electrodes 6 mm dia. 3 mm from tubes.			2, 7
Damianidis, Karayiannis, Collins and Allen [116]	R114	9 low fin tubes, fin root dia. 17.6 mm, fin height 0.5 mm, fin pitch 0.88 mm.		2.5	2, 7, 8
		9 smooth tubes o.d. 19.1 mm.		1.3	2, 7, 8
		Perforated brass plate and rod electrode			

Notes:
(1) Dielectrophoresis analyzed.
(2) D.c. electric field.
(3) A.c. electric field.
(4) Effect of EHD on minimum film boiling.
(5) A.c. electric field frequency varied.
(6) Electrically heated source.
(7) Fluid heated source.
(8) Ebullition initiated by EHD.
(9) High thermal capacity source.
(10) Fine wire mesh or array high voltage electrode.
(11) Observations of bubble dynamics.
(12) Correlation suggested.
(13) Enhancement by liquid jet (but bubble dynamics also affected).

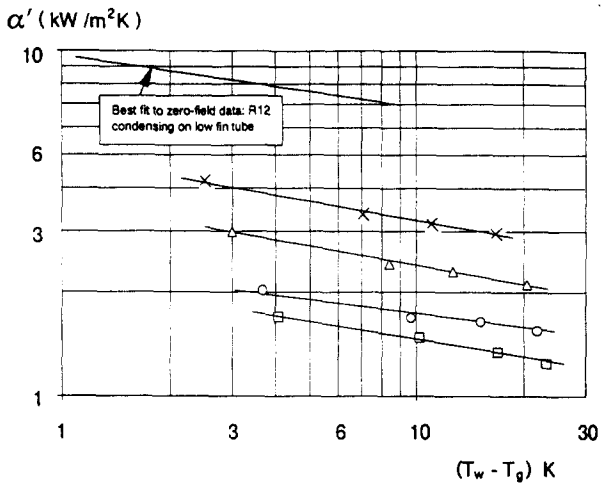

Fig. 3. EHD enhancement of R12 condensation with electrode voltages 20, 25, and 30 kV at outer surface of smooth horizontal tube compared with EHD-free smooth and low fin surface tubes ($T_g = 30°C$) [96].

enhancement was significant, see Fig. 7. No enhancement was obtained for the smooth tube bundle except in the convective regime. This was attributed to the electric field distribution. The electrode geometry used in ref. [115] resulted in radial electric field with the resultant EHD force pushing the bubbles away from the heated tube surface instead of on to the surface. This was not the case in the work reported by Ogata *et al.* [16]. They tested three different tube bundles boiling R123 and obtained significant EHD improvement in the heat transfer coefficient (seven times at 18 kV). Ogata *et al.* used steel rods and wires placed circumferentially and 3 mm away from the tubes as the electrodes. The non-uniformity of the resulting electric field moved the bubbles towards the tube surface and hence enhanced the heat transfer. The bubble movement in a low fin geometry, which has a beneficial effect on the heat transfer surface, was discussed earlier. Both research groups reported that EHD enhancement of boiling heat transfer in bundles is as effective as on a single tube.

EHD boiling inside tubes was studied by Yabe *et al.* [119] using a 10 mm inside diameter cupronickel tube and a coaxial cylindrical perforated steel electrode of 5 mm diameter. The EHD behaviour of the non-azeotropic mixture of R123 and R134a was studied. An enhancement of almost three times was obtained in the heat transfer coefficient. A change in the flow pattern from stratified to annular was also observed. The enhancement ratio decreased as the mass flux through the tube increased. The researchers also verified that for a given thermal duty, the pressure drop across the evaporator is the same, with or without EHD.

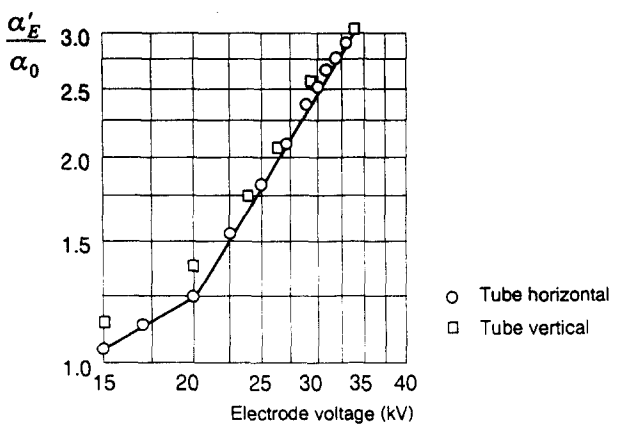

Fig. 4. EHD enhancement of R114 condensation at outer surfaces of vertical and horizontal tubes ($\Delta T = 25$ K, $T_0 = 90°C$) [96].

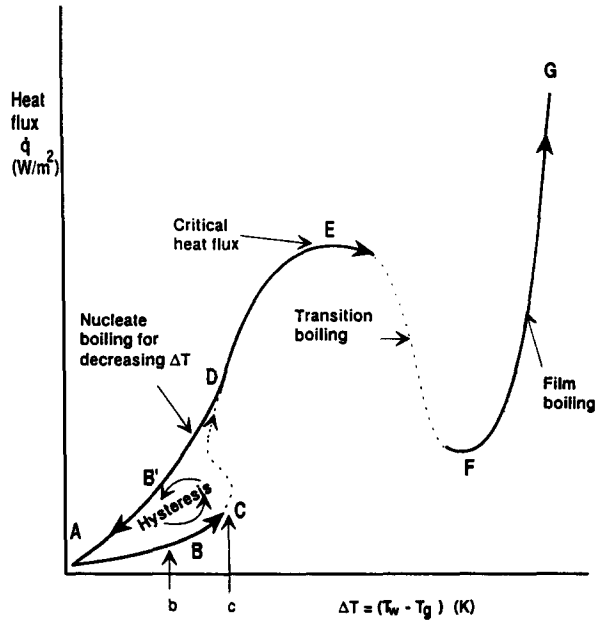

Fig. 5. The boiling curve showing heat flux density vs degree of ΔT.

5. EHD ENHANCEMENT CORRELATIONS

Correlation of heat transfer data in terms of non-dimensional quantities for specific geometries has long proved a valuable tool for heat exchanger design.

(a) *Single phase*

Correlations of experimental EHD results for systems with geometric similarity in terms of non-dimensional variables have been used for over 40 yr, since Kronig and Schwartz [120] postulated the superposition of the effects of normal natural convection and those of dielectrophoresis, expressed as Nusselt number, Nu, and its change, ΔNu, respectively. ΔNu gave a linear

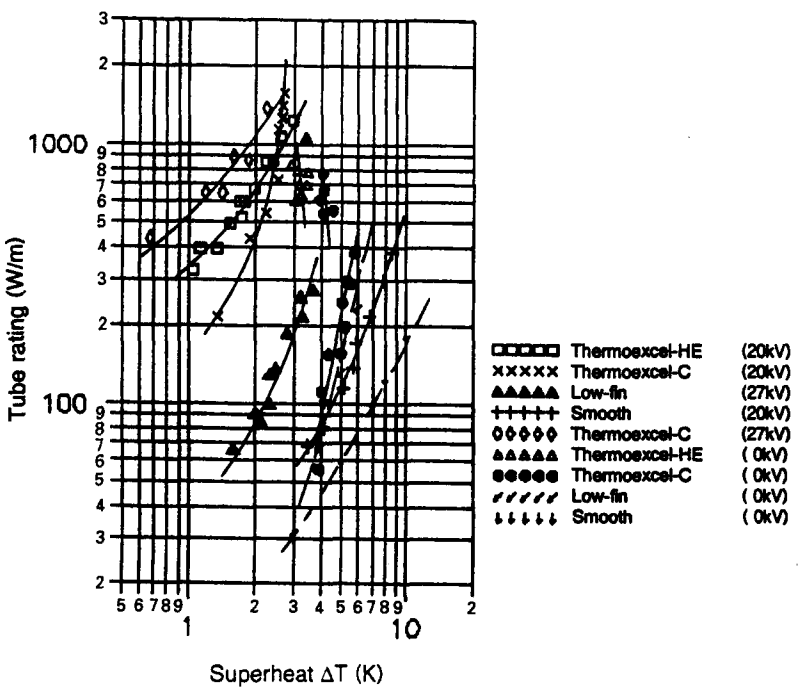

Fig. 6. Single tube rating vs degree of ΔT for various tube surfaces and R114 (Tube o.d. $\approx$ 19 mm).

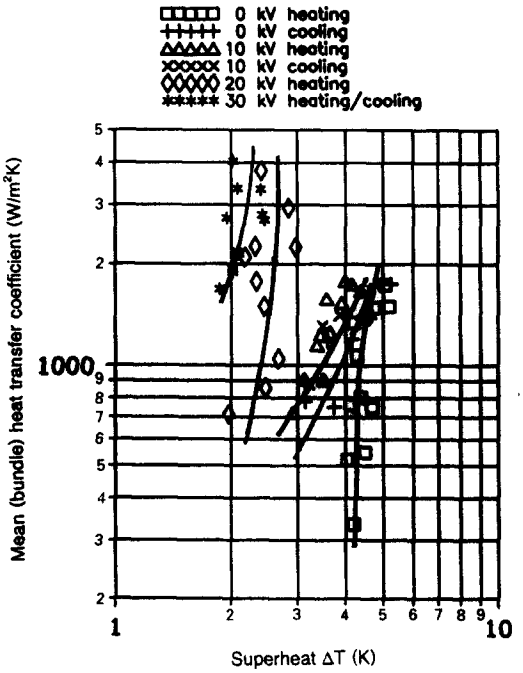

Fig. 7. EHD heat transfer enhancement in a nine low fin tube evaporator with R114 ($T_s = 30°C$).

log–log plot against *El*, an electric influence number, multiplied by the fluid Prandtl number, *Pr*. *El* is defined as

$$El = \frac{\rho \dfrac{d\epsilon}{dT} \ell^2 \Delta T E^2}{\mu^2} \tag{31}$$

and is closely related to the Grashof number, *Gr*, used to correlate natural convective heat transfer. In fact

$$El = Gr \frac{\left[\dfrac{E^2}{2}\dfrac{d\epsilon}{dT}\right]}{\rho \beta g \ell} \tag{32}$$

$$El = Gr\, A \tag{33}$$

say. A later modification due to Senftleben and Bültmann [121] proposes

$$Gr\, Pr\, A(1 + 0.00008A)$$

as the correlation variable. The correction to *El* is, however, small and usually of the same order as, or smaller than, the experimental error.

To allow for the effect of fluid electrical conductivity on electrophoresis, Turnbull [10] proposed an alternative electric influence number:

$$El' = \frac{\rho\epsilon \dfrac{1}{\sigma_e}\dfrac{d\sigma_e}{dT} \ell^2 \Delta T E^2}{\mu^2}. \tag{34}$$

He warned, however that successful correlation with respect to either *El* or *El'* is not a sufficient criterion to distinguish between electrophoretic and dielectrophoretic effects; this is best done by comparing a.c. and d.c. results.

Figure 8 shows results from ref. [45] for "Avtur" and from ref. [122] for transformer oil, correlated in terms of *Nu*, *Pr* and a voltage parameter,

$$\phi \sqrt{\frac{\epsilon\rho}{\mu}}.$$

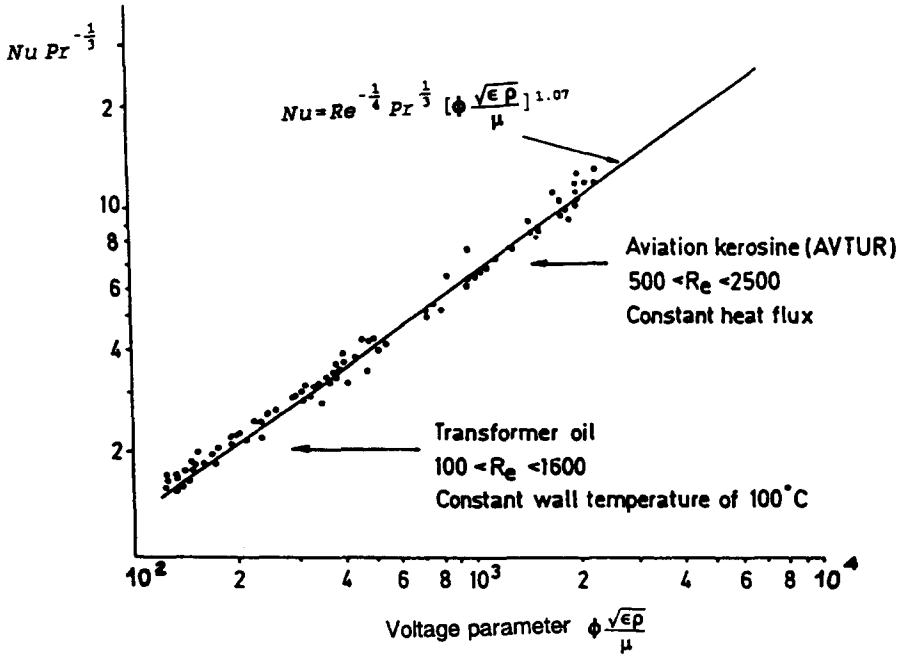

Fig. 8. Correlation of EHD single phase heat transfer for aviation kerosine and transformer oil [45].

To correlate corona wind results, Davidson *et al.* [123] have suggested using a dimensionless electric number:

$$Ne = \sqrt{\frac{i}{\eta D \rho \bar{v}^2}}, \tag{35}$$

where i is the ionization current, η is the ion mobility, D is the tube i.d. and ρ and $\bar{v}$ are fluid density and mean velocity, respectively, and this has been used successfully by Nelson *et al.* [36].

(b) *Condensation*

In the case of EHD-assisted condensation, correlation has been attempted from the earliest work. Having analyzed the disruption of the condensate film in terms of a perturbation wavelength λ^*, Choi and Reynolds [81] and later Choi [82] used this as the characteristic length in the Nusselt number, Nu', and modified Rayleigh number, Ra', for the correlation

$$Nu' = C_A (Ra')^{0.25}, \tag{36}$$

where C_A is an empirical constant and

$$Nu' = \alpha \frac{\lambda^*}{\lambda} \tag{37}$$

$$Ra' = \frac{F_\xi \rho (\lambda^*)^3 \Delta i'}{\lambda \mu \Delta T_{ln}}, \tag{38}$$

where λ and μ are fluid thermal conductivity and viscosity, respectively. ΔT_{ln} is the logarithmic mean value at ΔT,

$$F_\xi = \frac{3}{4\sigma}\left[\left(1 - \frac{\epsilon_s}{\epsilon_l}\right)^4 \epsilon_g^2 E_g^4\right], \tag{39}$$

σ being liquid surface tension, ϵ_g and ϵ_l permittivities of vapour and liquid, respectively, E_g the electric field strength in the vapour and

$$\Delta i' = i_{lg} + c_{pg}\Delta T + \tfrac{3}{8} c_{pl} \Delta T_{ln}, \tag{40}$$

where i_{lg} is the enthalpy of evaporation and c_{pg} and c_{pl} are specific heats of vapour and liquid, respectively. By contrast, Bologa and Didkovskiy [11] in their earlier work used the simpler relationship:

$$\frac{\alpha_E}{\alpha_0} = 0.28\left[\frac{E}{E_c}\right]^{2.5}, \tag{41}$$

where E_c is the electric field strength at which the EHD effect becomes significant ($E_c = 1.3$ MV/m). They also reported greater enhancement for polar fluids (diethyl ether) than non-polar (hexane, R113). They attributed this to the presence of free charges and the promotion of the electrophoretic force. However, in later work [85] they used the relatively complex correlation

$$\log\left[\frac{\alpha_E}{\lambda}\left(\frac{\nu^2}{g}\right)^{1/3}\right] \quad \text{vs} \quad \log\left[\frac{K^{1.2}\pi^{0.2}}{(Re')^{1/3}}\right],$$

where

$$K = \frac{\epsilon_g E_g^2 \ell}{\sigma_{lg}} \tag{42}$$

(the measure of the electric forces to the surface tension ratio),

$$\pi = \frac{\ell^2}{\tau\nu} \tag{43}$$

(the measure of the time ratio between damping of mechanical disturbances and relaxation time) and

$$Re' = \frac{\dot{q}h}{i_{lg}\rho\nu}, \tag{44}$$

the characteristic length ℓ being the annular gap, while h is the surface height and τ the charge relaxation time for the liquid. Subsequently [86], they correlated their own results together with those of Velkoff and Miller [80] and Smirnov and Lunev [87] in this way, but with the index of π decreased to 0.175, see Fig. 9. Smirnov and Lunev [87] themselves proposed the correlation of

$$\frac{Nu_E - C_B Nu_0}{C_C\left[\frac{D_i}{D_o}\right]^3};$$

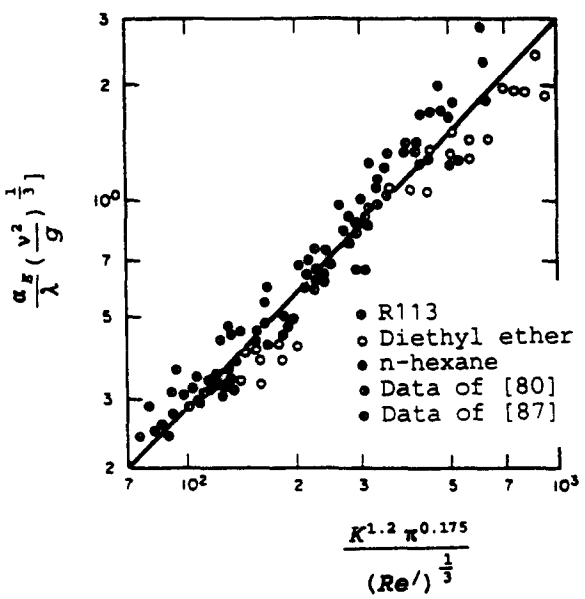

Fig. 9. Correlation of EHD condensation heat transfer [86].

Nusselt numbers using heat transfer surface height as characteristic vs Re'_E, where

$$Re'_E = \frac{h(\epsilon_l - \epsilon_g)E}{v\epsilon_l}\sqrt{\frac{\epsilon_0}{\rho}\left[1 - \left(\frac{E_c D_i}{gD_o}\right)^2\right]}. \tag{45}$$

In spite of these later refinements, Cooper [96] found the original [81, 82] correlation valid for his own results, as well as for those of Didkovsky and Bologa [86]. With $C_A = 0.35$ (rather than 0.5 as originally proposed) the scatter is about $\pm 30\%$ for $F_\xi > 60{,}000$, which is no worse than with the correlations suggested in refs [86] and [87].

(c) *Boiling*

In boiling, the effect of the electric field upon the maximum ($\dot{q}_c$) and minimum (point F in Fig. 5) heat fluxes and the correlation of this effect has received particular attention. In the case of $\dot{q}_c$ this is important since it could represent the maximum allowable heat transfer. Increasing the heat flux to a value greater than $\dot{q}_c$ gives rise to very high ΔT that can lead to burn-out. Johnson [124] considered the influence of the electric field on hydrodynamic stability. He amended the hydrodynamic theory of boiling heat transfer to include the effect of a perpendicular electric field across the vapour–liquid interface that exists at the maximum and minimum heat flux and correlated the ratio $(\dot{q}_c)_E/(\dot{q}_c)_0$ as a function of fluid properties and electric field strength. One resulting equation for maximum heat flux condition was

$$\frac{(\dot{q}_c)_E}{(\dot{q}_c)_0} = \left[\frac{f_1\left[1 + \sqrt{1 + \dfrac{3(\rho_l - \rho_g)g\sigma}{f_1^2}}\right]}{\sqrt{3(\rho_l - \rho_g)g\sigma}}\right]^{1/2}, \tag{46}$$

where

$$f_1 = \left(\frac{\epsilon_g}{\epsilon_l}\right)\frac{[\epsilon_l - \epsilon_g]^2}{\epsilon_l + \epsilon_g}E^2. \tag{47}$$

A similar relationship was recommended for the minimum heat flux.

$$\frac{(\dot{q}_{min})_E}{(\dot{q}_{min})_0} = \frac{\left[\dfrac{f_2}{3} + \dfrac{2(\rho_l - \rho_g)g\sigma}{f_2 + \sqrt{f_2^2 + 3(\rho_l - \rho_g)g\sigma}}\right]^{1/2}}{[\frac{4}{3}(\rho_l - \rho_g)g\sigma]^{1/4}}, \tag{48}$$

where

$$f_2 = \left(\frac{\epsilon_l}{\epsilon_g}\right)\frac{[\epsilon_l - \epsilon_g]^2}{\epsilon_l + \epsilon_g}E^2. \tag{49}$$

These relationships were compared both in Johnson [124] and Winer [14] with the limited experimental results of Winer (for a radial field a cylindrical heat transfer surface and R114) and found to be in good agreement, Fig. 10. In addition, Johnson stated that electric fields of the order of ~ 1 MV/m are required for any significant effect.

Jones and Schaeffer [105] modified the Zuber hypothesis [125, 126] for the minimum film boiling point to account for a strong EHD coupling at the vapour–liquid interface forming on a fine wire. They identified three electroquasistatic regimes based on the relation of the electric field frequency and the fluid charge relaxation time. The first regime was that of an insulating liquid where the frequency is much greater than the inverse charge relaxation time. Following the intermediate regime the third regime refers to a sufficiently conductive fluid. Jones and Schaeffer obtained relationships similar to those above for insulating and conducting fluids. Their theoretical results for $(\dot{q}_{min})_E/(\dot{q}_{min})_0$ were somewhat below the experimental results for R113 boiling on a fine wire.

Berghmans [127] considered a flat heater located in a conducting liquid and performed a stability analysis including the effect of a uniform d.c. field. This analysis resulted in

$$\dot{q}_c = \rho_g^{1/2} i_{lg} \frac{\pi}{2}\frac{1}{8}\left(\frac{1}{3}\right)^{1/4}(\sigma\rho_l g)^{1/4}\left[\frac{G^2}{\sqrt{3}B} + \left(\frac{G^4}{3B^2} + 1\right)^{1/2}\right]^{1/2}, \tag{50}$$

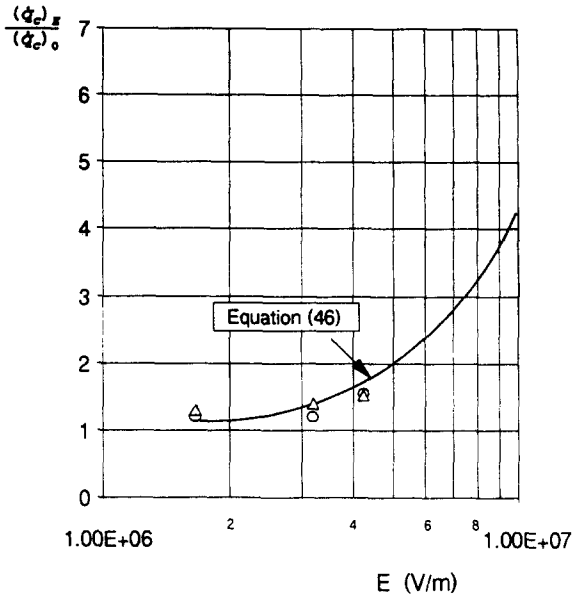

Fig. 10. Comparison of the predicted effect of an electric field on maximum heat flux with experimental results [124].

where $G^2 = \epsilon_g E^2 d/\sigma$ is the ratio of the electric forces to the surface tension forces and $B^2 = \rho_l g d^2/\sigma$, B^2 being the Bond number which is the ratio of inertia to surface tension forces; d is the vapour film thickness which can be obtained from experiments. This equation compared well with the data of Markels and Durfee [20]. Markels and Durfee used isopropyl alcohol and distilled water, both being conducting liquids. A correction was made to allow for the cylindrical surface used in ref. [20]. The choice of d which varies in the experiment was considered to be a possible reason for any deviations of the theory from the experiment.

Zhorzholiani and Shekriladze [112] have successfully correlated their own results and those of Markels and Durfee [20] on a log plot of

$$\frac{(\dot{q}_c)_E}{(\dot{q}_c)_0} \quad \text{vs} \quad \frac{F_D + g\rho}{g\rho}.$$

This is seen in Fig. 11. In their analysis, Zhorzholiani and Shekriladze considered F_D as both the second and third components of the EHD force in equation (1). It is the volume force density obtained from their summation. In their experiments they considered both neutral (n-pentane, benzene) and polar (acetone) fluids.

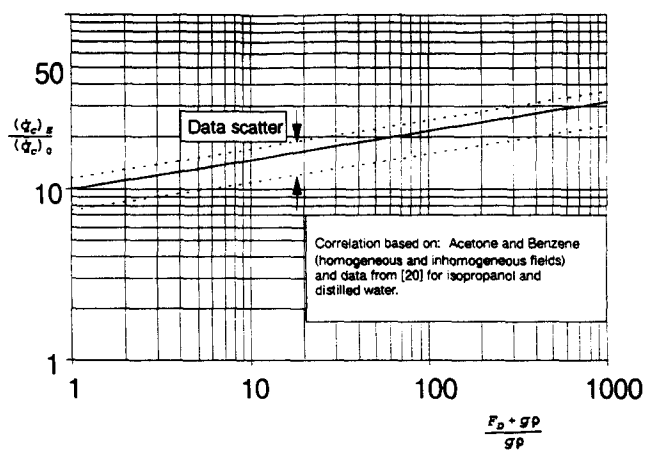

Fig. 11. Correlation of EHD increase in critical heat flux [112].

More recently, Cooper [128] has proposed a model for EHD nucleate boiling that leads to the relationship

$$\frac{\alpha_E}{\alpha_0} N^{-n/2} = 0.3 Re_0^{-0.16}, \tag{51}$$

where n is found experimentally,

$$N = 1 + \left[\frac{1.5\epsilon_l(\epsilon_g - \epsilon_l)}{(\epsilon_g + 2\epsilon_l)g(\rho_l - \rho_g)}\right]\nabla E^2 \tag{52}$$

and

$$Re_0 = \frac{\dot{q}}{i_{lg}\mu_l}\sqrt{\frac{\sigma}{g(\rho_l - \rho_g)}}. \tag{53}$$

Equation (51) correlates the results of refs [20, 67, 99, 100, 111] to within $\pm 10\%$ for the majority of 37 observations graphed with only one outside $\pm 30\%$, see Fig. 12.

6. ELECTRODE SYSTEMS

Little of the work reviewed here claims to include proposals for the practical implementation of EHD enhancement in industrial plant, although most commend its potential for material savings, etc. However, in Japan, Yabe *et al.* [88, 91] describe recent work on the development of electrode systems for vertically aligned shell/tube condensers with particular applications in heat pump systems. The electrode took the form of varying pitch helices. These use EHD to remove the condensate film at points along the tube surfaces and to spray it on to the high voltage electrodes down which it trickles. Figure 13 shows one such arrangement, optimized with respect to extraction and removal angles (defined in the figure) and dimensions.

This arrangement has been incorporated into a 50 kW, 102 tube, EHD condenser for a prototype heat pump and has shown heat transfer coefficient improvements compared with no EHD of about six times for R114 [94]. (This work has also confirmed the validity of applying EHD results obtained in single-tube rigs to multi-tube heat exchangers.) To enhance boiling, the Japanese have also employed EHD pumping [114] or fine wire electrode systems [108] but neither has been applied in the prototype heat pump mentioned above. By contrast, in the U.K., the electrode geometry developed by Allen and Cooper [129] specifically for shell/tube heat exchangers and shown in Fig. 14 is mechanically simpler and more compact. It has been shown to be effective for both condensation and boiling. It comprises a combination of rod and perforated plane electrodes, giving a fair approximation to the field that can be produced if a concentric cylinder was placed

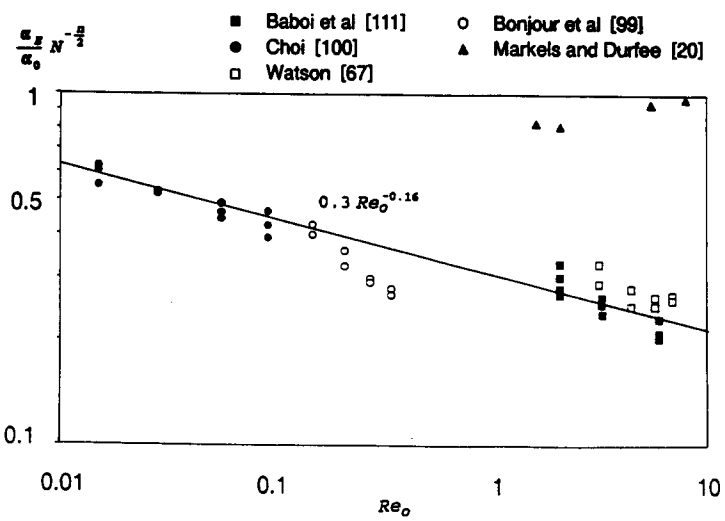

Fig. 12. Correlation of EHD nucleate boiling heat transfer rate [128].

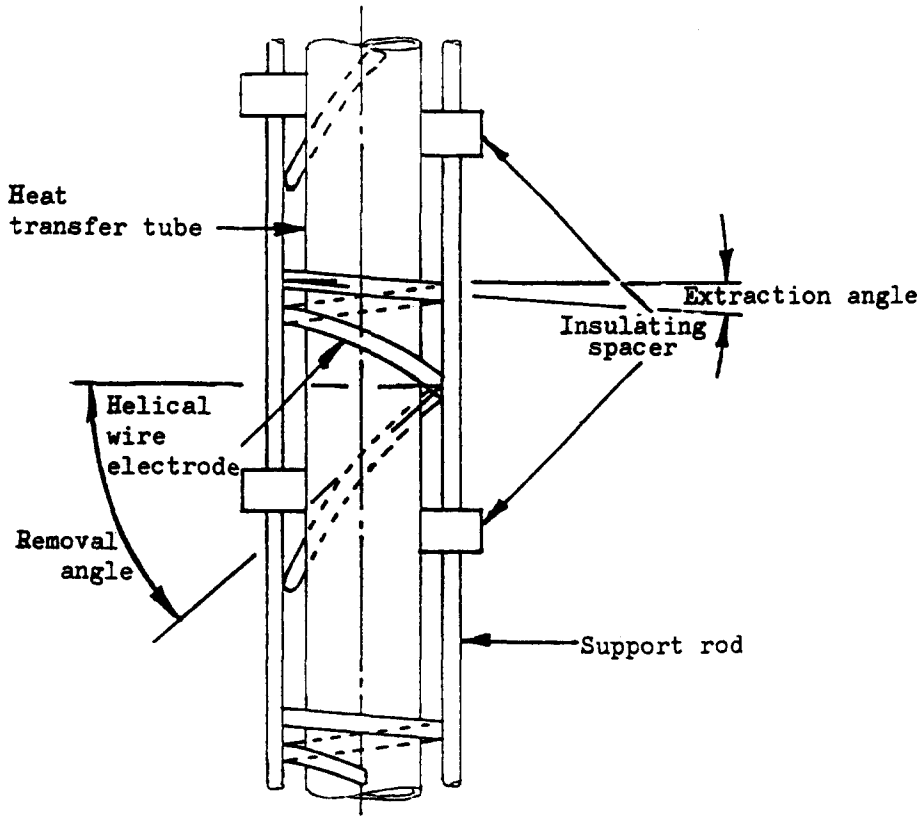

Fig. 13. Electrode system for EHD enhancement of vertical condenser tubes [88, 91].

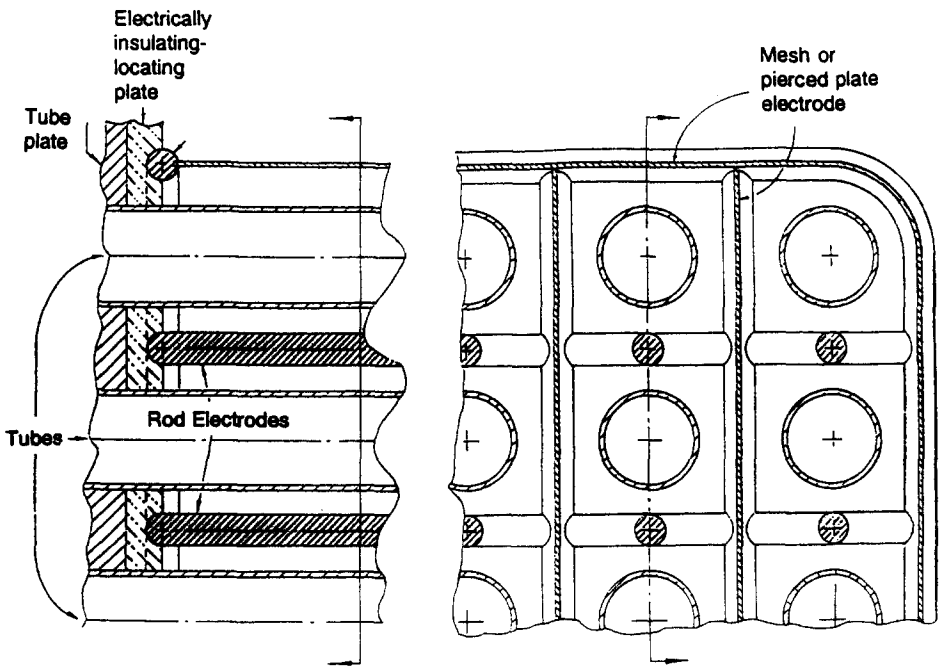

Fig. 14. Electrode system for EHD enhancement of vertical and horizontal shell/tube condensers and boilers as proposed by ref. [129].

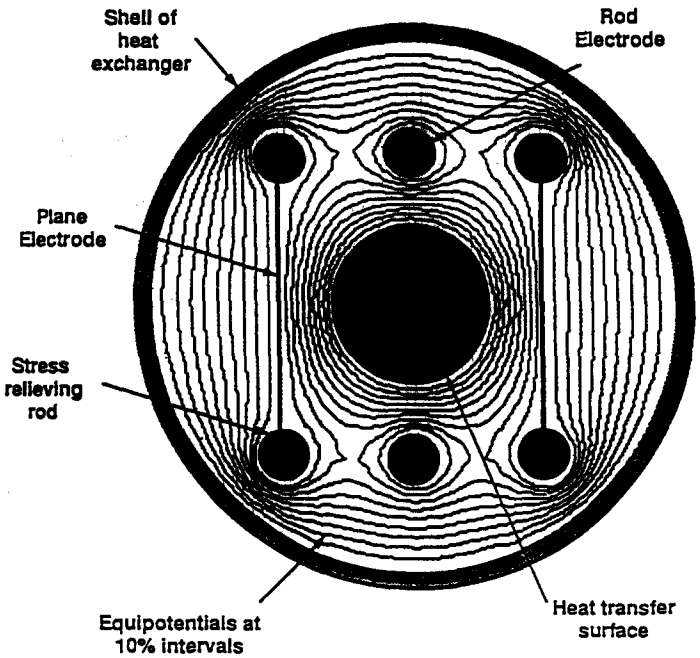

Fig. 15. Distribution of electric field strength for rod and plane electrode system [130].

around each tube, as shown in Fig. 15 from ref. [130]. Figure 16 shows an arrangement described by Poulter and Allen [131] for applying an electric field at the inner surface of tubes.

7. DISCUSSION

Clearly, in single phase heat transfer, certain geometries (e.g. inside tubes with axial electrodes) and certain fluids (e.g. "polar" ones) are especially amenable to EHD enhancement. Although many of the geometries investigated may seem to give little engineering design data, the fluids

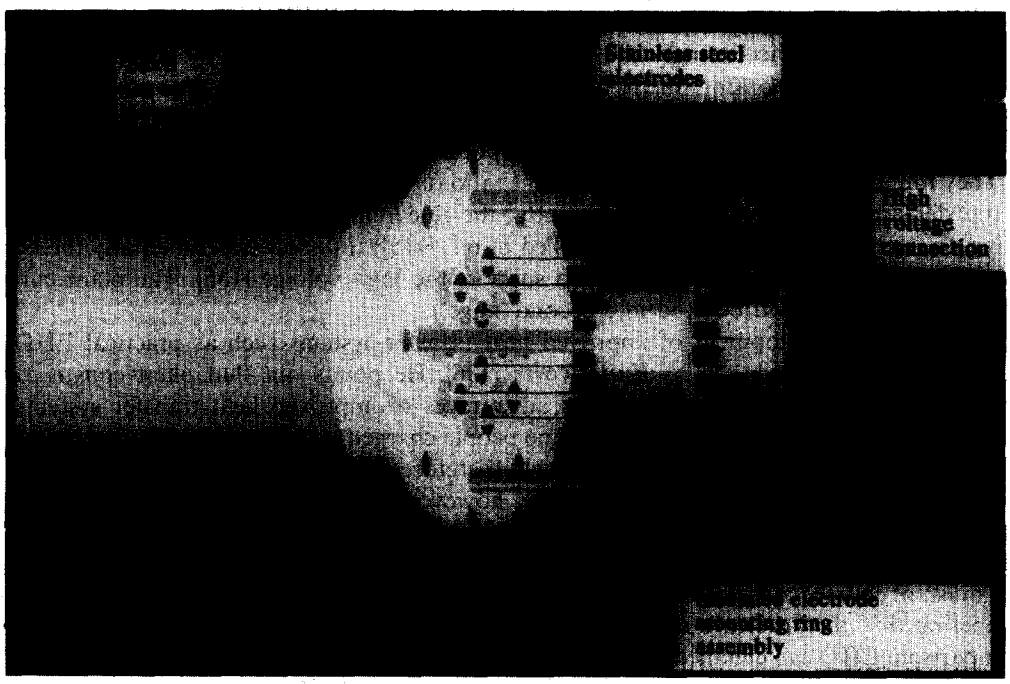

Fig. 16. Electrode system designed and used to apply an electric field at the inner surface of tubes [131].

investigated in them give an indication of their EHD potential. Evidently, all common gases are amenable to corona wind generation. Fluids shown to have been amenable to low energy consumption EHD enhancement are included in Tables 1–3.

What direction should single-phase EHD enhancement research and development take? Two clues are embedded in the data presented here. First, the possibility noted in ref. [39] that a mixture of d.c. with superimposed a.c. stress can give a more reliable and repeatable electrophoretic effect. Secondly, that, as mentioned in ref. [58], low frequency "square wave" a.c. stress can have the same effect. This is borne out by optical evidence of the behaviour of dielectric fluids in an electric field. Many publications [24, 49, 51, 68] give this and probably the most apposite to the present argument is ref. [51] which, using shadowgraphs, proves the region disturbed by the field developing from the (positive) earthed electrode across the duct width.

What next in two-phase EHD heat transfer? The clues to the answer lie in the work of Ogata *et al.* [16], Damianidis *et al.* [115] and the more recent work of Xu *et al.* [132]. An optimization strategy in the design of EHD multi-tube evaporators has to be identified. Cornwell [133, 134] examined the existence of sliding bubbles in boiling outside tube bundles and reported on their influence on heat transfer. He stated that the heat transfer mechanism involves the process of bubbles sliding on the surface disrupting the boundary layer and continued by saying that this effect is more important than evaporation. He offered as evidence, among other observations, the variation of the local heat transfer coefficient on a single tube, i.e. higher α on the tube sides. Cornwell concluded that the mechanism of heat transfer at the sliding bubbles is dominated by the influx of liquid to the layer under the bubble as it slides along the surface. The authors believe that the above arguments must be considered, if one is to optimize the electrode/heat transfer surface. The electrode/tube geometry has to be such that bubbles are directed along the heat transfer surface. In the current work of Xu *et al.* different electrode/heat transfer geometries are examined. A finite element model has been developed to calculate the EHD force on a bubble using equation (22). The findings of the mathematical simulation will be verified in a smooth tube bundle using R11 and R123. In the case of low-fin or other tubes with enhanced surfaces, the local non-uniformity of the electric field will enhance heat transfer rates significantly, as discussed earlier.

The isolated response of the heat exchanger has been examined and, as indicated above, will still attract the attention of researchers. The integrated response of the thermal system and the beneficial effects of EHD (size, cost) should also be considered. Ogata *et al.* [16] modelled an organic Rankine cycle (ORC) power generation system with waste energy as the heat source and a heat pump using waste heat from urban rivers as the heat source. Both systems used R123. The required heat transfer area of the ORC, and accordingly the cost, decreased by 20% on the inclusion of the EHD enhancement at the evaporator. In the heat pump system, at constant heat transfer, the cost of the EHD evaporator was about 10% lower than a conventional (low-fin) one. The COP of the EHD system was 7.9% higher. Damianidis *et al.* [115] reported on a model of a typical water chiller using R22. They found that the use of an enhancement ratio of 1.8 gave a 15% reduction in the required heat transfer area of the evaporator. Currently, the research team at South Bank University is working on a prototype water chiller (modelled in ref. [115]) to assess experimentally the benefits of the use of EHD. (R22 was found not to support the high voltage [135]. The plant currently utilizes R12 and R123 will be used in a second stage.)

Obstacles to the development of improved heat transfer systems such as practical EHD heat exchangers have been reviewed by Butterworth [136]. He points out that plant construction is organized so that "people who can see the advantages of improved heat transfer systems, and indeed benefit from them, may not be the same people charged with designing those systems. The latter have no incentive to make changes and will therefore design the system the same way as they did the last time". He concludes that "there are, however, possible ways to improve the shell and tube, and we should use as much ingenuity to making further developments in the shell and tube as we have to developing alternative types".

One must, of course, consider the relative merits of EHD and "passive" enhancement techniques, remembering that the latter are effective only in the nucleate boiling region (up to E in Fig. 5). By comparison, EHD can enhance every part of the boiling curve. Kajikawa *et al.* [137] gave results for tubes comparable in size to those used by the present authors [13, 15, 89, 115, 116, 135] coated

with a "Highflux"-type porous copper coating and with fine metal fibre used in an R114 boiler. Apart from a graph showing a step increase of about three times in tube row heat transfer coefficients as the warm water temperature increased to 30°C and above (no refrigerant saturation temperature is quoted), which is described as "peculiar", there is no data on hysteresis. Maximum α values of about 11 kW/m^{2}K can be construed from their results. Results for other refrigerants are given by Czikk *et al.* [138] (R11, maximum α 42.5 kW/m^{2}K) for coated tubes and by Arai *et al.* [139] (R12, maximum α 24 kW/m^{2}K) for "Thermoexcel-E" with no mention of hysteresis. Hysteresis with a porous metallic coating has, however, been thoroughly investigated by Bergles and Chyu [140] for the case of R113. They found that about 8 K superheat was needed for ebullition, which then increased α by about 20 times, a degree of boiling curve hysteresis that they describe as "dramatic". They conclude that although greatly enhancing heat transfer, a porous metallic matrix surface is to be expected to give hysteresis and that this effect had not been presented previously in the literature.

Regarding enhanced condensation, Arai *et al.* [139] report improvements using R12 and "Thermoexcel" tube amounting to between 25 and 70%. This, however, could well be no better than the improved performance of tube banks given by EHD condensate stripping. The excellent boiling performance of EHD, combined with a low fin surface, is probably connected with Cornwell's observation [134] that "this may become churn flow where bubbles coalesce to form elongated vapour regions". The electric field combines with buoyancy and the tube profile shape to produce the elongation.

Lastly, the many other possibilities inherent in EHD enhancement should not be ignored. For example, the work of Rutkowski [113] suggests that the evaporation of recalcitrant cryogenic liquids may well be assisted by EHD. Bologa and Savin [141] described how an electric field can be applied for intensifying and controlling the process of heat and mass transfer in zones of evaporation, condensation and transport processes in heat pipes. In another paper, Savin *et al.* [142] found that the rate of evaporation can increase significantly with the application of electric fields. They reported that at 30 kV the rate of evaporation of liquid nitrogen increased by 6.5 times its rate at zero-field. Higher increases were obtained for R113. Thornton [143] gives a general account of the application of electrical energy to a variety of chemical and physical rate processes, including heat and mass transfer.

8. CONCLUSIONS

The authors hope that they have justified the following conclusions:

1. Single phase heat transfer rates can be significantly enhanced using electric fields. Corona wind and electrophoresis give the highest enhancement ratios, although consideration must be given in the former case to the power consumption and in the latter to the purity and polarity of the medium and the possibility of charge injection.
2. EHD pumps, although not very efficient, can find practical use due to the absence of moving parts.
3. EHD can be applied effectively to the enhancement and control of condensation and boiling of very many fluids.
4. In condensers, the EHD effect upon smooth tubes cannot compete with the degree of enhancement offered by a "low-fin" surface. Nevertheless, it is expected to improve the performance of banks of low fin tubes.
5. In boilers, the EHD effect can increase $\dot{q}_c$ and eliminate both boiling hysteresis and decreases in the boiling heat transfer coefficient due to transition and film boiling.
6. Electrode systems have been developed for the application of EHD in shell/tube heat exchangers, although optimization is yet to be completed.

Acknowledgements—The results given in Figs 3, 4, 6, 7 and 12 are from work supported, successively, by the Science and Engineering Research Council and the British Technology Group. The authors wish also to acknowledge the assistance of their research students R. K. Al-Dadah, Y. Yan and Y. Xu in preparing the figures.

REFERENCES

1. D. A. Reay, Heat transfer enhancement—a review of techniques and their possible impact on energy efficiency in the U.K. *Heat Recovery Systems & CHP* **11,** 1–40 (1991).
2. A. E. Bergles, The challenge of enhanced heat transfer with phase change. *Trans. VII Congresso Nazionale sulla Transmissione del Calore*, Florence, 1989, pp. 1–12.
3. A. E. Bergles, Techniques to augment heat transfer. In *Handbook of Heat Transfer Applications* (Edited by W. M. Rohsenow, J. P. Hartnett and E. N. Ganic), 2nd Edn. McGraw-Hill, New York (1985).
4. S. Yilmaz, J. J. Hwalek and J. W. Westwater, Pool boiling heat transfer performance for commercial enhanced tube surfaces. ASME, Paper No. 80-HT-41, 1980.
5. L. D. Landau and E. M. Lifshitz, *Electrodynamics of Continuous Media.* Pergamon, New York (1963).
6. H. A. Pohl, *Dielectrophoresis—The Behavior of Neutral Matter in Nonuniform Electric Field.* Cambridge University Press, Cambridge (1978).
7. T. B. Jones, Electrohydrodynamically enhanced heat transfer in liquids—a review. *Adv. Heat Transfer* **14,** 107–148 (1978).
8. F. P. Grosu and M. K. Bologa, Similarity criteria for convective heat exchange in an electric field. *Appl. Elec. Phenom. (USSR)* **20,** 120–125 (1968).
9. A. Yabe, Active heat transfer enhancement by applying electric fields. *Proc. ASME/JSME Thermal Engng Joint Conf.*, 1991 (Edited by J. R. Lloyd and Y. Kurosaki), pp. xv–xxiii.
10. R. J. Turnbull, Electroconvective instability with a stabilizing temperature gradient II. Experimental results. *Phys. Fluids* **11,** 2597–2603 (1968).
11. M. K. Bologa and A. B. Didkovskiy, Enhancement of heat transfer in film condensation of vapors of dielectric liquids by superposition of electric fields. *Heat Transfer—Soviet Res.* **9**(1), 147–151 (1977).
12. J. L. Olinger and C. P. Colver, A study of the effect of a uniform electric field on nucleate and film boiling. *Chem. Engng Prog. Symp. Ser.* **67,** 19–29 (1971).
13. T. G. Karayiannis, M. W. Collins and P. H. G. Allen, Electrohydrodynamic enhancement of nucleate boiling heat transfer in heat exchangers. *J. Chem. Engng Commun.* **81,** 15–24 (1989).
14. M. Winer, An experimental study of the influence of a nonuniform electric field on heat transfer in a dielectric fluid, TRW Systems Report, Report No. EM17-14, 1967.
15. P. H. G. Allen and P. Cooper, The potential of electrically enhanced evaporators. *Proc. 3rd Int. Symp. on the Large Scale Application of Heat Pumps*, Oxford, U.K., 1987, pp. 221–229.
16. J. Ogata, Y. Iwafuji, Y. Shimada and T. Yamazaki, Boiling heat transfer enhancement in tube-bundle evaporators utilizing electric field effects. *ASHRAE Trans.* **98**(2), 435–444 (1992).
17. M. M. Ohadi, R. A. Papar, T. L. Ng, M. A. Faani and R. Radermacher, EHD enhancement of shell-side boiling heat transfer coefficients of R-123/oil mixture. *ASHRAE Trans.*, ibid, 427–434 (1992).
18. W. M. Rohsenow, Nucleation with boiling heat transfer. *Ind. Engng Chem.* **58**(1), 40–47 (1966).
19. W. M. Rohsenow, A method of correlating heat-transfer data for surface boiling of liquids. *Trans. Amer. Soc. Mech. Engrs* **74,** 969–976 (1952).
20. M. Markels and R. L. Durfee, The effect of applied voltage on boiling heat transfer. *AIChE J.* **10**(1), 106–109 (1964).
21. Anon. Developments to watch: a noiseless fan, with no moving parts. *Product Engng*, 10 October, 29 (1966).
22. R. E. Holmes and S. J. Basham, A dry cooling system for steam power plants. *Proc. 6th Intersociety Energy Conversion Eng. Conf.*, Boston, MA, 1971, pp. 1218–1228.
23. H. R. Velkoff, The effects of ionization on the flow and heat transfer of a dense gas in a transverse electrical field. *Proc. Heat Transfer and Fluid Mechanics Institute*, University of California, Berkeley (Edited by W. H. Giedt and S. Levy), pp. 260–275. Stanford University Press (1964).
24. R. A. Moss and J. Grey, Heat transfer augmentation by steady and alternating electric fields. *Proc. Heat Transfer and Fluid Mechanics Institute*, University of Santa Clara, 1966 (Edited by M. A. Saad and J. A. Miller), pp. 210–235.
25. F. P. Grosu and M. K. Bologa, The influence of electric fields on heat-exchange processes in gases. *Appl. Elec. Phenom. (USSR)* **5**(23), 350–356 (1968).
26. M. Robinson, Convective heat transfer at the surface of a corona electrode, *Int. J. Heat Mass Transfer* **13,** 263–274 (1970).
27. J. McDermott, High-voltage ionic discharges provide silent, efficient cooling. *Electronic Des.* **20** 30 September, 22–24 (1971).
28. T. Mizushina, H. Ueda, T. Matsumoto and K. Waga, Effect of electrically induced convection on heat transfer of air flow in an annulus. *J. Chem. Engng Japan* **9,** 97–102 (1976).
29. H. Windischmann, Investigation of corona-discharge cooling (CDC) of a horizontal plate under free convection, *AIChE Symp. Series* **138,** 23–30 (1974).
30. J. Yamaga and M. Jido, Corona discharge cooling technique, U.S. Patent No. 3,938,345, 1976.
31. K. G. Kibler and H. G. Carter, Localised corona discharge. U.S. Patent No. 4,015,658, 1977.
32. A. Yabe, Y. Mori and K. Hijikata, Heat transfer augmentation around a downward-facing flat plate by non-uniform electric fields. *Proc. 6th Int. Heat Transfer Conf.*, 1978, Paper M-20, Vol. 3, pp. 171–176.
33. A. Yabe, Y. Mori and K. Hijikata, EHD study of the corona wind between wire and plate electrodes. *AIAA J.* **16**(4), 340–345 (1978).
34. H. R. Velkoff and R. Godfrey, Low-velocity heat transfer to a flat plate in the presence of a corona discharge in air. *J. Heat Transfer* **101,** 157–163 (1979).
35. Y. Tada, A. Takimoto and Y. Hayashi, Heat transfer enhancement in a convective field by applying ionic wind. *Proc. ASME/JSME Thermal Engng Joint Conf.*, 1991 (Edited by J. R. Lloyd and Y. Kurosaki), Vol. 3, pp. 9–14.
36. D. A. Nelson, M. M. Ohadi, S. Zia and R. L. Whipple, Electrostatic effects on heat transfer and pressure drop in cylindrical geometries, ibid, pp. 33–39.
37. E. Schmidt and W. Leidenfrost, Der Einfluss elektrischer Felder auf den Wärmetransport in flüssigen elektrischen Nichtleitern, *Forsch. auf dem Geb. des Ing.-wes* **19**(3), 65–80 (1953).
38. E. Schmidt and W. Leidenfrost, Der Wärmetransport in flüssigen elektrischen Nichtleitern unter dem Einfluss elektrischer Felder, *Chemie-Ing.-Techn.* **26,** 35–38 (1954).

39. P. H. G. Allen, Electric stress and heat transfer, *Brit. J. Appl. Phys.* **10,** 347–351 (1959).
40. S. Mascarenhas, Y. Mascarenhas, M. Ferreira De Souza and R. F. Rabello, Thermal conduction of liquid dielectric under the influence of electric fields (fatty acids). *An. Acad. Brasil Ci.* **28,** 95–98 (1956).
41. H. Senftleben and P. Schnabel, Der Einfluss von Raumladungen in hochisolierenden Flüssigkeiten auf den Wärmeübergang unter Wirkung elektrischer Felder. *Z. Phys.* **170,** 82–92 (1962).
42. J. M. Care and D. W. Swan. Some transient phenomena in heat transfer resulting from electric stress. *Brit. J. Appl. Phys.* **14,** 263–266 (1963).
43. J. E. Porter and R. Poulter, Electrothermal convection effects with laminar flow heat transfer in an annulus. *Proc. 4th Int. Heat Transfer Conf.*, Paris, 1970, Paper FC3.7, Vol. 2.
44. D. C. Newton and P. H. G. Allen, Senftleben effect in insulating oil under uniform electric stress. *Lett. Heat Mass Transfer* **4,** 9–16 (1977).
45. R. Poulter and I. A. Miller, Heat transfer enhancement in shell/tube heat exchangers employing electrostatic fields. *Proc. Ist U.K. Nat. Heat Transfer Conf.*, Leeds, 1984, Vol. 2, pp. 707–716.
46. J. L. Fernandez and R. Poulter, Radial mass flow in electrohydrodynamically enhanced forced heat transfer in tubes. *Int. J. Heat Mass Transfer* **30,** 2125–2135 (1987).
47. S. Mascarenhas, The action of homogeneous electric fields upon the heat transmission of liquid dielectrics. *An. Acad. Brasil. Ci.* **28,** 99–105 (1956).
48. U. T. Borbulya, I. A. Kojuhar and M. K. Bologa, Electroconvection heat transfer with dielectric fluids. *Arch. Academy of Moldavian S.S.R.* **2,** 90–93 (1965).
49. M. J. Gross and J. E. Porter, Electrically induced convection in dielectric liquids. *Nature* **212**(5068), 1343–1345 (1966).
50. J. E. Porter and R. B. Smith, The effect of a transverse electrostatic field on laminar flow heat transfer in a rectangular duct. *Proc. 5th Int. Heat Transfer Conf.*, Tokyo, 1974, Paper FC 5.4, Vol. 2, pp. 198–202.
51. T. Fujino, Y. Yokoyama and Y. H. Mori, Augmentation of laminar forced-convection heat transfer by the application of a transverse electric field. *Trans. ASME J. Heat Transfer* **111,** 345–351 (1989).
52. H. Ishiguro, S. Nagata, A. Yabe and H. Nariai, Augmentation of forced-convection heat transfer by applying electric fields to disturb flow near a wall. *Proc. ASME/JSME Thermal Engng Joint Conf.*, 1991 (Edited by J. R. Lloyd and Y. Kurosaki), Vol. 3, pp. 25–31.
53. V. Stach, Influence of electric field on the cooling gas flow in a nuclear reactor. *Int. J. Heat Mass Transfer* **5,** 445–456 (1962).
54. F. Berger and L. Derian, The influence of an electric field on the heat transfer to CO_2 at high and low pressure in a nuclear reactor. *Proc. 3rd Int. Conf. on the Peaceful Uses of Atomic Energy*, Geneva, 1964, Vol. 8, pp. 355–363.
55. F. Berger and L. Derian, The influence of an electric field on the heat transfer to gaseous coolants in a nuclear reactor. *Acta Technica CSAV* **3,** 312–335 (1965).
56. J. M. Coulson and J. E. Porter, The effects of electric fields on transport phenomena. *Trans. Inst. Chem. Engrs* **44,** T388–T394 (1966).
57. R. Schnurmann and M. G. C. Lardge, Enhanced heat flux in non-uniform electric fields. *Proc. R. Soc. Lond. A* **334,** 71–82 (1973).
58. P. Cooper and P. H. G. Allen, The Senftleben effect in cross-flow heat exchange and the part played by electronic conduction. *PhysicoChem. Hydrodynam.* **4,** 85–101 (1983).
59. N. F. Baboi, M. K. Bloga and K. N. Semenov, The influence of electric fields on heat transfer in liquids and gases. *Appl. Elec. Phenom. (USSR)* **1,** 46–57 (1965).
60. K. N. Semenov, N. F. Baboi and M. K. Bologa, Effective influence of electro-magnetic field on heat transfer in gases and liquids. *Academic News of the Moldavian SSR* **2,** 82–89 (1965).
61. H. Senftleben, Die Einwirkung elektrischer und magnetischer Felder auf des Wärmeleitvermögen von Gasen. *Phys. Z.* **32,** 550 (1931).
62. H. Senftleben and W. Braun, Der Einfluss elektrischer Felder auf den Wärmestrom in Gasen. *Z. Phys.* **102,** 480–506 (1936).
63. S. Y. Wang, M. W. Collins and P. H. G. Allen, Prediction of the effect of electrohydrodynamic (EHD) enhancement of fluid flow and heat transfer. *Proc. Ist Int. Conf. on Advanced Computation Methods in Heat Transfer*, Portsmouth, 1990, Vol. 2, pp. 231–238.
64. P. H. G. Allen, Heat transfer at high voltage. *Elec. Times* **139,** 321–322 (1961).
65. G. Ahsmann and R. Kronig, The influence of electric fields on the convective heat transfer in liquids. *Appl. Sci. Res. A* **2,** 235–244 (1950). (Correction: **3,** 83/84, 1951.)
66. H. J. De Haan, The influence of electric fields on the convective heat transfer in liquids II. *Appl. Sci. Res. A* **3,** 85–88 (1951).
67. P. K. Watson, Influence of an electric field upon the heat transfer from a hot wire to an insulating liquid. *Nature* **189,** 563–564 (1961).
68. K. H. Weber and G. H. Halsey, Free convection in electric fields. *Proc. Heat Transfer and Fluid Mechanics Institute*, pp. 97–100. Stanford University Press (1953).
69. S. D. Savkar, Dielectrophoretic effects in laminar forced convection between two parallel plates. *Phys. Fluids* **14,** 2670–2679 (1971).
70. A. J. Oliver, The effect of electric fields on heat transfer and its relevance to the CEGB SF_6 power cable, CERL Lab Note TPRD/L/2398/N82, 1983.
71. J. Seyed-Yagoobi, J. C. Chato, J. M. Crowley and P. T. Krein, Induction electrohydrodynamic pump in a vertical configuration: Part 1—Theory. *Trans. ASME J. Heat Transfer* **111,** 664–669 (1989).
72. J. Seyed-Yagoobi, J. A. Castañeda and J. E. Bryan, Theoretical analysis of ion-drag pumping. *Proc. IEEE-IAS Annual Meeting*, 1992.
73. M. Sato, A. Yabe and T. Taketani, Heat transfer enhancement by applying an electro-hydrodynamical pump utilizing dielectrophoretic force. *Proc. ASME/JSME Thermal Engng Joint Conf.*, 1991 (Edited by J. R. Lloyd and Y. Kurosaki), Vol. 3, pp. 3–8.
74. J. Seyed-Yagoobi, J. C. Chato, J. M. Crowley and P. T. Krein, Induction electrodynamic pump in a vertical configuration: Part 2—Experimental study. *Trans. ASME J. Heat Transfer* **111,** 670–674 (1989).

75. B. J. Bohinsky and J. Sayed-Yagoobi, Induction electrohydrodynamic pumping. Selecting an optimum working fluid. *Proc. IEEE-IAS Annual Meeting*, 1990, pp. 795–801.
76. J. Seyed-Yagoobi, A theoretical study of induction electrohydrodynamic pumping in outer space. *Trans. ASME J. Heat Transfer* **112,** 1095–1097 (1990).
77. J. E. Bryan and J. Seyed-Yagoobi, Experimental study of ion-drag pumping using various working fluids. *IEEE Trans. Electrical Insulation* **26,** 647–655 (1991).
78. J. A. Castañeda and J. Seyed-Yagoobi, Electrohydrodynamic pumping of Refrigerant 11. *Proc. IEEE-IAS Annual Meeting*, 1991, pp. 500–503.
79. J. E. Bryan and J. Seyed-Yagoobi, An experimental investigation of ion-drag pump in a vertical and axisymmetric configuration. *IEEE Trans. on Industry Applications* **28,** 310–316 (1992).
80. H. R. Velkoff and J. H. Miller, Condensation of vapour on a vertical plate with a transverse electrostatic field. *Trans. ASME J. Heat Transfer* **87,** 197–201 (1965).
81. H. Y. Choi and J. M. Reynolds, Study of electrostatic effects on condensing heat transfer, Air Force Technical Report AFFDL-TR-65-51, Air Force Flight Dynamics Laboratory, Wright-Patterson Air Force Base, Ohio, 1965.
82. H. Y. Choi, Electrohydrodynamic condensation heat transfer, *Trans. ASME J. Heat Transfer* **90,** 98–102 (1968).
83. R. E. Holmes and A. J. Chapman, Condensation of Freon-114 in the presence of a strong nonuniform alternating electric field. *Trans. ASME J. Heat Transfer* **92,** 616–620 (1970).
84. A. K. Seth and L. Lee, The effect of an electric field in the presence of noncondensable gas on film condensation heat transfer. *Trans. ASME J. Heat Transfer* **96,** 257–258 (1974).
85. A. B. Didkovskii and M. K. Bologa, Intensification of heat exchange upon condensation of a vapour in an electric field. *High Temp.* **16,** 490–496 (1978).
86. A. B. Didkovsky and M. K. Bologa, Vapour film condensation heat transfer and hydrodynamics under the influence of an electric field. *Int. J. Heat Mass Transfer* **24,** 811–819 (1981).
87. G. F. Smirnov and V. G. Lunev, Heat transfer during condensation of vapour of dielectric liquids in electric fields. *Appl. Elec. Phenom. (USSR)* **2,** 37–42 (1978).
88. A. Yabe, K. Kikuchi, T. Taketani, Y. Mori and K. Hijikata, Augmentation of condensation heat transfer by applying non-uniform electric fields. *Proc. 7th Int. Heat Transfer Conf.*, 1982, Vol. 5, pp. 189–194.
89. P. Cooper and P. H. G. Allen, The potential of electrically enhanced condensers. *Proc. 2nd Int. Symp. on the Large Scale Application of Heat Pumps*, Oxford, U.K., 1984, pp. 295–309.
90. J. Trommelmans and J. Berghmans, Influence of electric fields on condensation heat transfer of non-conducting fluids on horizontal tubes. *Proc. 8th Int. Heat Transfer Conf.*, 1986, Vol. 6, pp. 2969–2974.
91. A. Yabe, T. Taketani, K. Kikuchi, Y. Mori and H. Maki, Augmentation of condensation heat transfer by applying electro-hydro-dynamical pseudo-dropwise condensation, ibid, pp. 2957–2962.
92. M. K. Bologa, I. K. Savin and A. B. Didkovsky, Electric-field-induced enhancement of vapor condensation heat transfer in the presence of a non-condensable gas. *Int. J. Heat Mass Transfer* **30**(8), 1577–1585 (1987).
93. C. Damianidis, M. W. Collins, T. G. Karayiannis and P. H. G. Allen, EHD effects in condensation of dielectric fluids. *Proc. 2nd Int. Symp. on Condensers and Condensation*, Bath, U.K., 1990, pp. 505–518.
94. K. Yamashita, M. Kumagai, S. Sekita, A. Yabe, T. Taketani and K. Kikuchi, Heat transfer characteristics of an EHD condenser. *Proc. ASME/JSME Thermal Engng Joint Conf.*, 1991 (Edited by J. R. Lloyd and Y. Kurosaki), Vol. 3, pp. 61–67.
95. G. F. Smirnov and I. I. Lukanov, Study of heat transfer from Freon-11 condensing on a bundle of finned tubes. *Heat Transfer—Soviet Research* **4**(3), 51–56 (1972).
96. P. Cooper, Electrically enhanced heat transfer in the shell/tube heat exchanger, PhD Thesis, University of London, 1986.
97. L. W. Chubb, Improvements relating to methods and apparatus for heating liquids. U.K. Patent No. 100,796, (1916).
98. L. Bochirol, E. Bonjour and L. Weil, Exchanges thermiques-Etude de l'action de champs electriques sur les transferts de chaleur dans les liquides bouillants. *C.R. Heb. des Seances de l'Acad. des Sciences (Paris)* **250,** 76–78 (1960).
99. E. Bonjour, J. Verdier and L. Weil, Electroconvection effects on heat transfer. *Chem. Engng Progr.* **58**(7), 63–66 (1962).
100. H. Y. Choi, Electrohydrodynamic boiling heat transfer, PhD Thesis, Dept. of Mech. Eng., M.I.T., 1962.
101. A. K. Jalaluddin and D. B. Sinha, Effect of an electric field on the superheat of liquids, *Nuovo Cimento* **26** (supplement), Series X, 234–237 (1962).
102. M. Markels and R. L. Durfee, Studies of boiling heat transfer with electric fields. Part I. Effect of applied a.c. voltage on boiling heat transfer to water in forced convection. *AIChE J.* **11**(4), 716–719 (1965).
103. R. F. Lovenguth and D. Hanesian, Boiling heat transfer in the presence of nonuniform, direct current electric fields. *Ind. Engng Chem. Fundam.* **10**(4), 570–576 (1971).
104. D. K. Basu, Effect of electric field on boiling hysteresis in carbon tetrachloride. *Int. J. Heat Mass Transfer* **16,** 1322–1324 (1973).
105. T. B. Jones and R. C. Schaeffer, Electrohydrodynamically coupled minimum film boiling in dielectric liquids. *AIAA J.* **14**(12), 1759–1765 (1976).
106. T. B. Jones and K. R. Hallock, Surface wave model of electrohydrodynamically coupled minimum film boiling. *J. Electrostatics* **5,** 273–284 (1978).
107. V. A. Zheltukin, Y. K. Solomatnikov, D. M. Mikhaylov and A. G. Usmanov, Effect of electric-field frequency on heat transfer. *Heat Transfer—Soviet Research* **10**(6), 10–13 (1978).
108. H. Kawahira, Y. Kubo and T. Yokoyama, The effect of an electric field on boiling heat transfer of Refrigerant 11. *Proc. IEEE/IAS Annual Meeting*, Atlanta, 1987, pp. 1446–1454.
109. R. A. Blachowicz, B. W. Brooks and K. B. Tan, Boiling heat transfer in an electric field. *Chem. Engng Sci.* **35,** 761–762 (1980).
110. V. Asch, Electrokinetic phenomena in boiling "Freon-113". *J. Appl. Phys.* **37**(7), 2654–2658 (1966).
111. N. F. Baboi, M. K. Bologa and A. A. Klyukanov, Some features of ebullition in an electric field. *Appl. Elec. Phenom. (USSR)* **20,** 126–141 (1968).
112. A. G. Zhorzholiani and I. G. Shekriladze, Study of the effect of an electrostatic field on heat transfer with boiling dielectric fluids. *Heat Transfer—Soviet Research* **4**(4), 81–98 (1972).
113. J. Rutkowski, The influence of electric field on heat transfer in boiling cryogenic liquid. *Cryogenics* **17,** 242–243 (1977).

114. A. Yabe and H. Maki, Augmentation of convective and boiling heat transfer by applying an electro-hydrodynamical liquid jet. *Int. J. Heat Mass Transfer* **31**(?), 407–417 (1988).
115. C. Damianidis, T. G. Karayiannis, R. K. Al-Dadah, R. W. James, M. W. Collins and P. H. G. Allen, EHD boiling enhancement in shell and tube evaporators and its application in refrigeration plants. *ASHRAE Trans.* **98**(2), 462–472 (1992).
116. C. Damianidis, M. W. Collins, T. G. Karayiannis and P. H. G. Allen, EHD enhancement of heat transfer in evaporators and condensers. *Proc. 11th Int. Symp. of Heating, Refrigerating and Air Conditioning*, Interklima 91, Zagreb, 1991, pp. 10–26.
117. Electrohydrodynamic (EHD) Effects on Condensing and Evaporating Freons. Video held by ASME Heat Transfer Films Library, Mechanical and Aerospace Engineering, The University of Tennessee, Knoxville, TE, 37996–2210.
118. Y. Y. Yan, T. G. Karayiannis, P. H. G. Allen, M. W. Collins and R. S. Neve, EHD enhancement of boiling heat transfer at low superheat surfaces in heat exchangers. *Proc. Eurotherm Seminar No. 33, Recent Developments in Heat Exchanger Technology*, Paris, 1993.
119. A. Yabe, T. Taketani, H. Maki, K. Takahashi and Y. Nakadai, Experimental study of electrohydrodynamically (EHD) enhanced evaporator for nonazeotropic mixtures. *ASHRAE Trans.* **98**(2), 455–461 (1992).
120. R. Kronig and N. Schwartz, On the theory of heat transfer from a wire in an electric field. *Appl. Sci. Res. A* **1**, 35–46 (1947).
121. H. Senftleben and E. Bültmann, Die Einwirkung elektischer Felder auf den Wärmeübergang in Gasen. *Z. für Phys.* **136**, 389–401 (1953).
122. J. L. Fernandez, Electrohydrodynamic enhancement of forced convective heat transfer in tubes, PhD thesis, University of Bristol, U.K., 1975.
123. J. H. Davidson, F. A. Kulacki and P. F. Dunn, Convective heat transfer with electric and magnetic fields. In *Handbook of Single-Phase Convective Heat Transfer* (Edited by S. Kakac, R. K. Shah and W. Aung), Chap. 9. Wiley, New York (1987).
124. R. L. Johnson, Effect of an electric field on boiling heat transfer. *AIAA J.* **6**(8), 1456–1460 (1968).
125. N. Zuber and M. Tribus, Further remarks on the stability of boiling heat transfer, UCLA Report No. 58-5, UCLA, Los Angeles, California, 1958.
126. N. Zuber, Hydrodynamic aspects of boiling heat transfer, ACE Rept No. AECU-4439, Atomic Energy Commission, 1959.
127. J. Berghmans, Electrostatic fields and the maximum heat flux. *Int. J. Heat Mass Transfer* **21**, 791–797 (1978).
128. P. Cooper, EHD enhancement of nucleate boiling. *Trans. ASME J. Heat Transfer* **112**, 458–464 (1990).
129. P. H. G. Allen and P. Cooper, Improvements in or relating to heat exchangers, U.K. Patent No. 8522680, 1985.
130. P. Cooper, Practical design aspects of EHD heat transfer enhancement in evaporators. *ASHRAE Trans.* **98**(2), 445–454 (1992).
131. R. Poulter and P. H. G. Allen, Electrohydrodynamically augmented heat and mass transfer in the shell/tube heat exchanger. *Proc. 8th Int. Heat Transfer Conf.*, San Francisco, 1986, Vol. 6, pp. 2963–2968.
132. Y. Xu, R. K. Al-Dadah, P. H. G. Allen and T. G. Karayiannis, Incorporation of EHD enhancement in heat exchangers. *ICHMT Int. Symp. on New Developments in Heat Exchangers*, Portugal, 1993.
133. K. Cornwell, The influence of bubbly flow on boiling from a tube in a bundle. *Proc. Eurotherm No. 8, Advances in Pool Boiling Heat Transfer*, Paderborn, Germany, 1989, pp. 177–184.
134. K. Cornwell, The role of sliding bubbles in boiling on tube bundles. *Proc. 9th Int. Heat Transfer Conf.*, Israel, 1990, Vol. 3, pp. 455–460.
135. T. G. Karayiannis, R. K. Al-Dadah, R. W. James and P. H. G. Allen, Electrohydrodynamic boiling heat transfer enhancement in heat exchangers. Paper 93-WA/HT-35, ASME Winter Annual Meeting, New Orleans, U.S.A., 1993.
136. D. Butterworth, Changes in heat exchangers for process applications: incentives and barriers. *Heat Transfer Engng* **8**(4) 19–22 (1987).
137. T. Kajikawa, T. Agawa, H. Takazawa, M. Amano, K. Nishiyama and T. Homma, Studies on OTEC power system characteristics and enhanced heat transfer performance. *Proc. 6th OTEC Conf.*, Washington USA, Paper 11-5, 1979.
138. A. M. Czikk, C. F. Gottzmann, E. G. Ragi, J. G. Withers and E. P. Habdas, Performance of advanced heat transfer tubes in refrigerant-flooded liquid coolers. *ASHRAE Trans.* **76**(1), 96–119 (1970).
139. N. Arai, T. Fukushima, A. Arai, T. Nakajima, K. Fujie and Y. Nakayama, Heat transfer tubes enhancing boiling and condensation in heat exchangers of a refrigerating machine. *ASHRAE Trans.* **83**(2), 58–70 (1977).
140. A. E. Bergles and M. C. Chyu, Characteristics of nucleate pool boiling from porous metallic coatings. *Trans. ASME J. Heat Transfer* **104**, 279–285 (1982).
141. M. K. Bologa and I. K. Savin, Electrohydrodynamic heat pipes. *7th Int. Heat Pipe Conf.*, Minsk, 1990, B14P.
142. I. K. Savin, M. K. Bologa and V. P. Korovkin, Effect of an electric field on the rate of heat and mass exchange during evaporation. *Electronnaya Obrabotka Materialov* **6**, 52–54 (1986).
143. J. D. Thornton, The applications of electrical energy to chemical and physical rate processes. *Rev. Pure Appl. Chem.* **18**, 197–218 (1968).